Supplementary Materials for

Induced Adult Neurogenesis plus BDNF Mimicks the Effects of Exercise on Cognition in an Alzheimer's Mouse Model

Se Hoon Choi,[1] Enjana Bylykbashi,[1] Zena K. Chatila,[1] Star W. Lee,[2] Benjamin Pulli,[3] Gregory D. Clemenson,[2] Eunhee Kim,[1] Alexander Rompala,[1] Mary K. Oram,[1] Caroline Asselin,[1] Jenna Aronson,[1] Can Zhang,[1] Sean J. Miller,[1] Andrea Lesinski,[1] John W. Chen,[3] Doo Yeon Kim,[1] Henriette van Praag,[4] Bruce M. Spiegelman,[5] Fred H. Gage,[2] Rudolph E. Tanzi[1,*]

[*]Corresponding author. E-mail: tanzi@helix.mgh.harvard.edu

This PDF file includes:

Figures S1 to S23
Tables S1 to S10

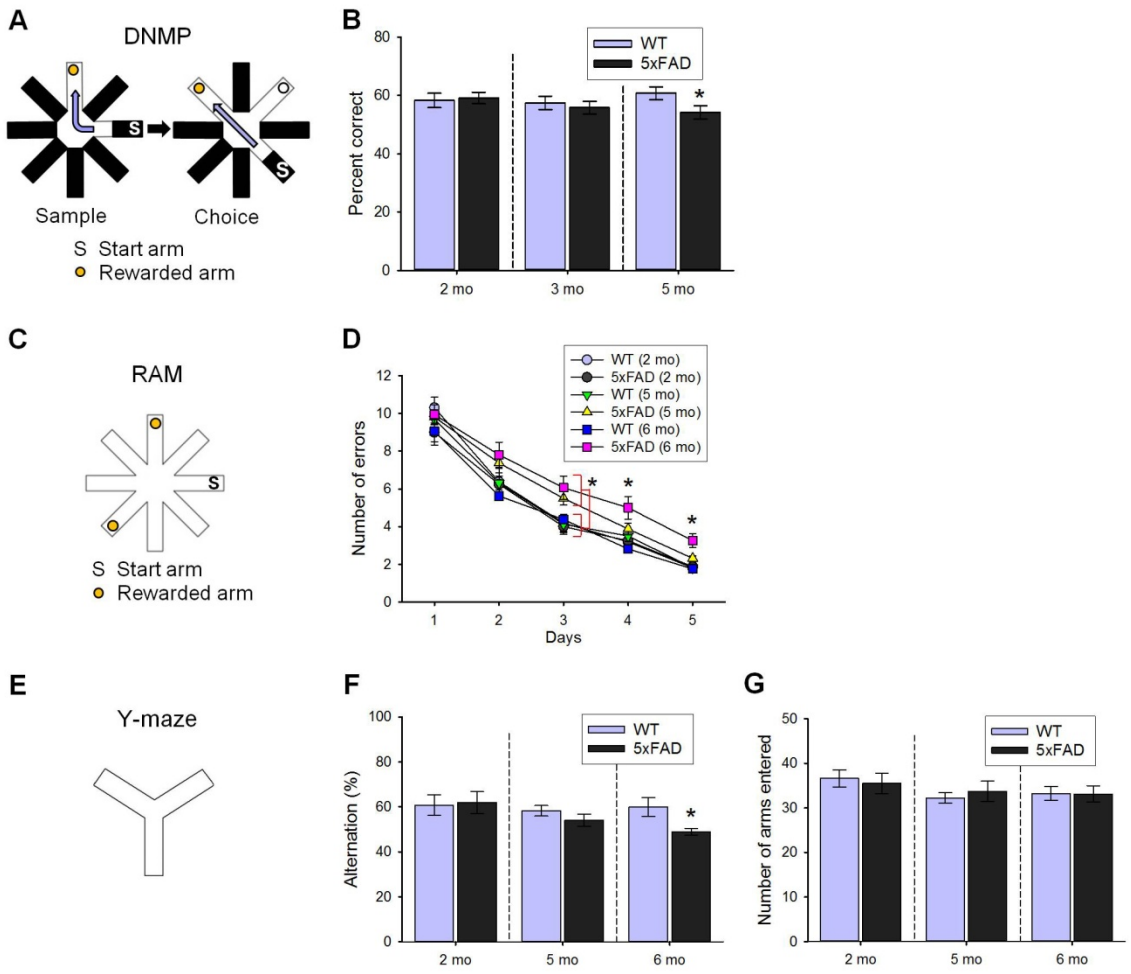

Fig. S1

Endogenous cognitive changes in 5×FAD mice.

(**A**, **B**) Schematic diagram of the delayed non-matching to place (DNMP) task in the 8-arm radial maze (RAM), which consisted of a sample phase and a choice phase (A), and quantification of percent correct during the choice phase of the DNMP task (B) (n = 10 per group). 5×FAD mice did not show any significant impairment in pattern separation when they were 2 and 3 months old, but showed impairment at 5 months compared to age-matched WT mice (*P < 0.05). (**C**, **D**) Schematic diagram of the RAM task (C) and mean number of errors of 2 trials per day as a function of 5 consecutive training days in the RAM task (D) (n = 8 per group). Both WT and 5×FAD mice showed a clear learning curve during the training sessions at the ages of 2, 5, and 6 months. A 2-way repeated measures ANOVA revealed significant effects for days ($F_{(4,168)}$ = 455.7, P < 0.01) and for groups ($F_{(5,42)}$ = 4.200, P < 0.01) but not for interaction ($F_{(20,168)}$ = 1.262, P = 0.221). Fisher's LSD post hoc tests revealed a significant increase in the number of errors in both 5- and 6-month-old 5×FAD mice when compared to the other groups on day 3 and in 6-month-old 5×FAD mice when compared to all other groups on days 4 and 5. *P < 0.05. (**E**-**G**) Schematic diagram of the Y-maze task (E) and spontaneous alternation behavior during an 8-min session in the Y-maze task (F). Data are presented as the percentage of

correct alternation to total arm entries (n = 8 per group). We tested spontaneous alternation in 2-, 5-, or 6-month-old WT and 5×FAD mice, and found that spontaneous alternation was impaired in 5×FAD mice beginning at 6 months (*$P < 0.05$). The total number of arms entered during the test was comparable for WT and 5×FAD mice at all the ages tested (G), indicating that 5×FAD mice had similar levels of motor and exploratory activity as WT mice at these ages.

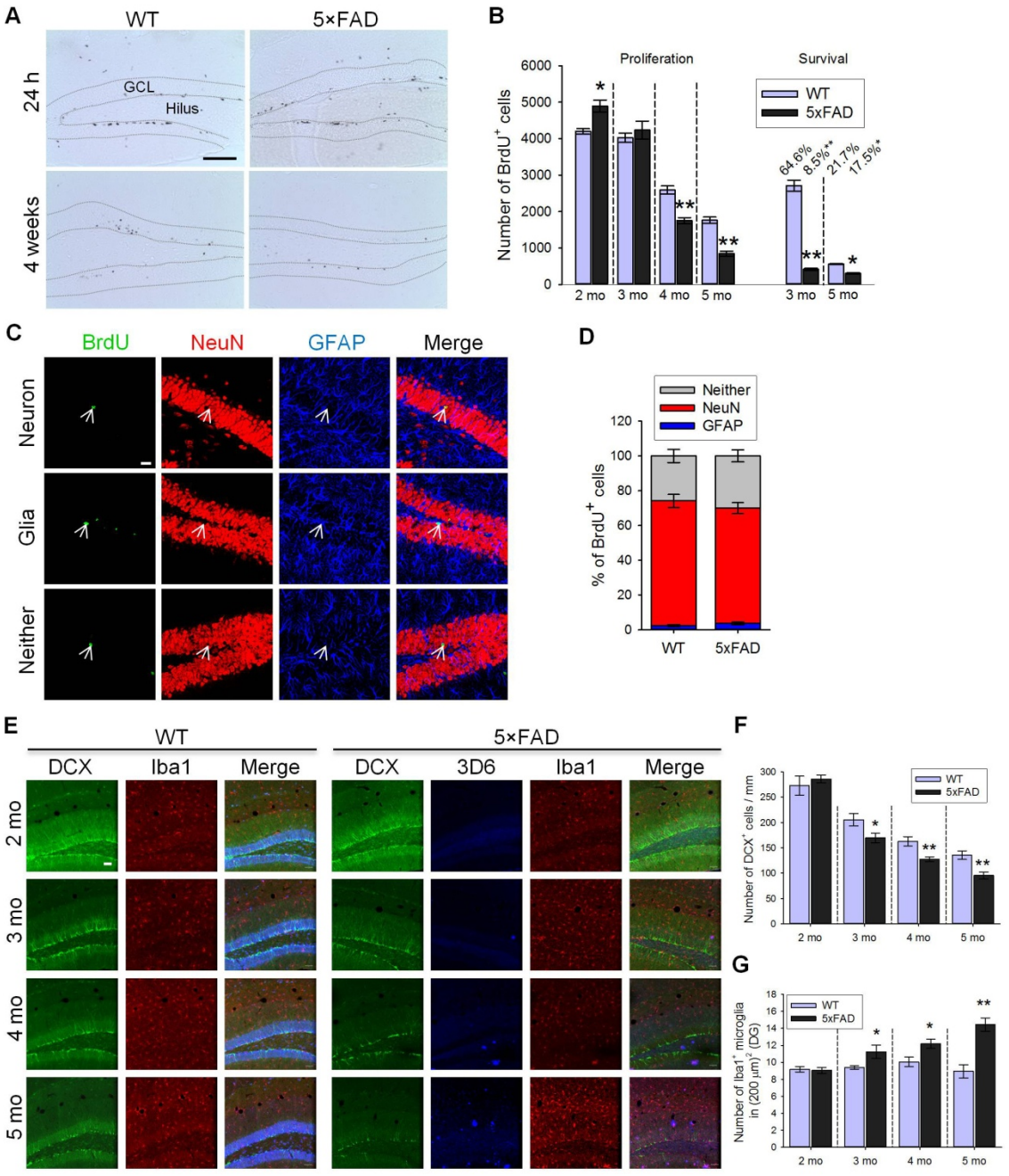

Fig. S2

Endogenous neurogenic changes and AD pathology in 5×FAD mice.

(**A**) Photomicrographs of $BrdU^+$ cells in the dentate gyrus (DG) of WT (left panels) and 5×FAD mice (right panels) at 24 h (upper panels) or 4 weeks (lower panels) after receiving the last BrdU injection at the age of 2 months. GCL, granule cell layer. Scale bar: 100 μm. (**B**) Quantification of $BrdU^+$ cells (n = 8 per group). mo, months. *P < 0.05, **P < 0.01 between WT and age-matched 5×FAD mice. To examine NPC proliferation, cohorts of 2-, 3-, 4-, or 5-month-old WT and 5×FAD mice received a single injection of BrdU daily for 3 days and were sacrificed 1 day after the last BrdU injection. Parallel

cohorts of 2- or 4-month-old mice were sacrificed 4 weeks after BrdU injection to determine the survival rate and differentiation of newborn NPCs. Examination of BrdU cells revealed a significant increase in NPC proliferation in 5×FAD mice compared to WT mice at the age of 2 months. However, this increase became indistinguishable at the 3 months of age. Meanwhile, NPC proliferation was significantly decreased in 4- and 5-month-old 5×FAD mice compared to age-matched WT mice. To provide a measure of cell survival during the 4-week post-BrdU injections, the number of $BrdU^+$ cells at 4-weeks post-BrdU injection was expressed as a percentage of the number of cells present at the 24 hours post-BrdU injections (indicated by % above the bars in the survival graph). This analysis revealed that a significantly lower fraction of $BrdU^+$ cells survived in 5×FAD mice compared to WT mice at both the 3- and 5-months of age. The absolute numbers of surviving $BrdU^+$ cells were significantly decreased in 5×FAD mice compared to WT mice at both ages. (**C**) Representative confocal microscope images of $BrdU^+$ cells in brain slices of 5×FAD mice. To determine the phenotypes of the $BrdU^+$ cells, triple-labeling confocal immunohistochemical analysis was performed using an antibody against BrdU (green), an antibody against the mature neuron-specific protein NeuN (red), and an antibody against the astrocyte GFAP (blue). The merged images of the three labels demonstrate cells with neuronal (upper panels) or glial (middle panels) properties or neither (lower panels). Arrows indicate the position of $BrdU^+$ cells. Scale bar: 20 μm. (**D**) Percentage of $BrdU^+$ cells colabeled with NeuN or GFAP or neither. No significant differences were observed in the fraction of $BrdU^+$ cells that were colabeled with NeuN or GFAP between WT and 5×FAD mice at 5-months old, suggesting that neuronal commitment of newborn NPCs was not altered in 5×FAD mice, at least up to these ages. (**E**) Representative confocal microscope images of DCX^+ neurons (green), $Iba1^+$ microglia (red), $NeuN^+$ mature neurons (blue in WT mice), and $3D6^+$ Aβ plaques (blue in 5×FAD mice) at the ages of 2, 3, 4, or 5 months. mo, months. Scale bar: 50 μm. 5×FAD mice exhibited slight Aβ deposition in the hippocampus, detected by 3D6 antibodies specific for an epitope at or near the amino terminus of Aβ, when they reached 3 months of age. A noticeable rise in Aβ deposition in the hippocampus began at 4 months of age, and 5-month-old mice showed extensive Aβ deposition in the hippocampus. (**F**) Quantification of DCX^+ cells (n = 8 per group). Analysis of DCX immunostaining uncovered a significant decrease in the total number of DCX^+ cells in 5×FAD mice compared to WT mice beginning at 3 months of age (*$P < 0.05$, **$P < 0.01$ between WT and age-matched 5×FAD mice). (**G**) Quantification of $Iba1^+$ microglia in the DG of WT and 5×FAD mice (n = 10 mice per group). Immunostaining for the microglia marker Iba1 revealed that the number of $Iba1^+$ microglial cells was, in general, proportional to Aβ deposition and was significantly increased in the hippocampus of 5×FAD mice beginning at 3 months of age (*$P < 0.05$, **$P < 0.01$ between WT and age-matched 5×FAD mice).

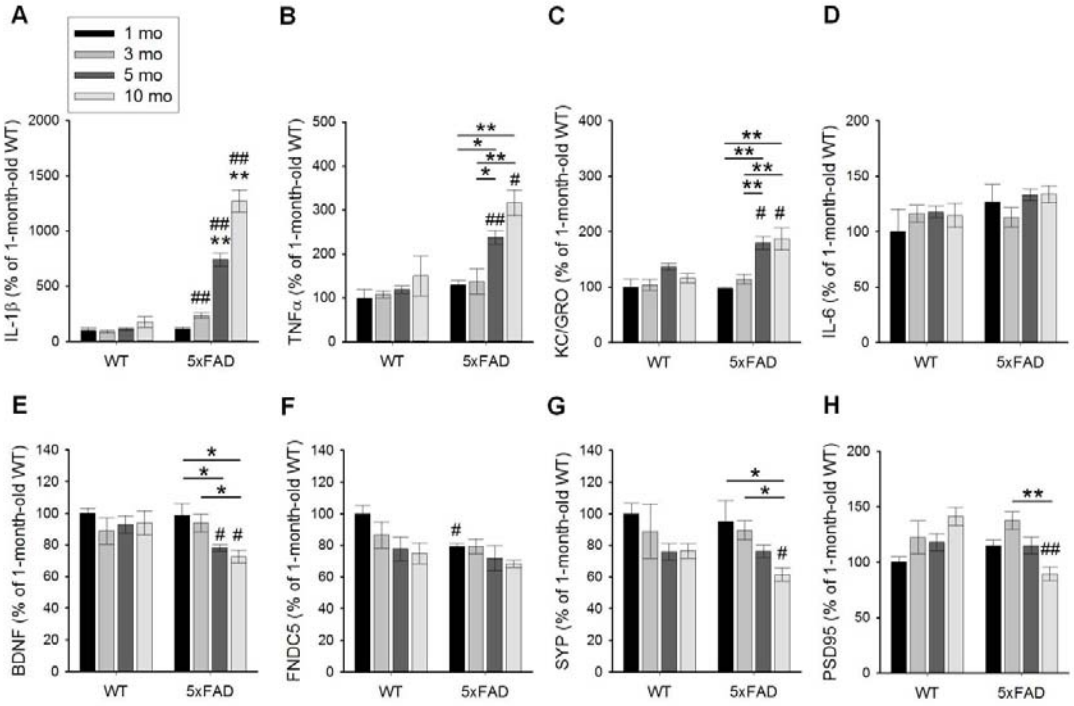

Fig. S3

Endogenous changes with age of interleukin-1β (IL-1β), tumor necrosis factor α (TNFα), Keratinocyte-derived chemokine (KC/GRO), IL-6, brain-derived neurotrophic factor (BDNF), fibronectin type III domain-containing protein-5 (FNDC5), synaptophysin (SYP) and post-synaptic density 95 (PSD95) in the hippocampus of WT and 5×FAD mice.

(**A**-**H**) Levels of hippocampal IL-1β (A), TNFα (B), KC/GRO (C), IL-6 (D), BDNF (E), FNDC5 (F), SYP (G) and PSD95 (H) in WT and 5×FAD mice at 1, 3, 5 and 10 months of age. Levels are presented as % of the levels in 1-month-old WT mice. In 5×FAD mice, the hippocampal levels of IL-1β, TNFα and KC/GRO were significantly increased beginning at 5 months of age. IL-6 levels were not changed. In addition, interferon γ (IFNγ), IL-2, IL-4, IL-5, IL-10, and IL-12p70 were measured, and the levels of each cytokine did not differ across all groups. BDNF levels were significantly decreased beginning at 5 months. FNDC5 levels were not changed with age in 5×FAD mice although 5×FAD mice showed lower levels compared to WT mice at 1 month of age. The levels of SYP were significantly lower in 10-month-old 5×FAD mice compared to 1- or 3-month-old 5×FAD mice and 10-month-old WT mice. PSD95 levels were significantly lower in 10-month-old 5×FAD mice compared to 3-month-old 5×FAD mice and 10-month-old WT mice. For IL-1β in 5×FAD mice, $F_{(3,20)} = 77.46$, $P < 0.01$. For TNFα in 5×FAD mice, $F_{(3,20)} = 15.57$, $P < 0.01$. For KC/GRO in 5×FAD mice, $F_{(3,20)} = 13.16$, $P < 0.01$. For BDNF in 5×FAD mice, $F_{(3,19)} = 5.658$, $P < 0.01$. For SYP in 5×FAD mice, $F_{(3,19)} = 4.314$, $P < 0.05$. For PSD95 in 5×FAD mice, $F_{(3,17)} = 8.969$, $P < 0.01$. *$P < 0.05$, **$P < 0.01$ between specified age group and all other ages in 5×FAD mice. $^{\#}P < 0.05$, $^{\#\#}P < 0.01$ between 5×FAD and age-matched WT mice. n = 5 or 6 per group.

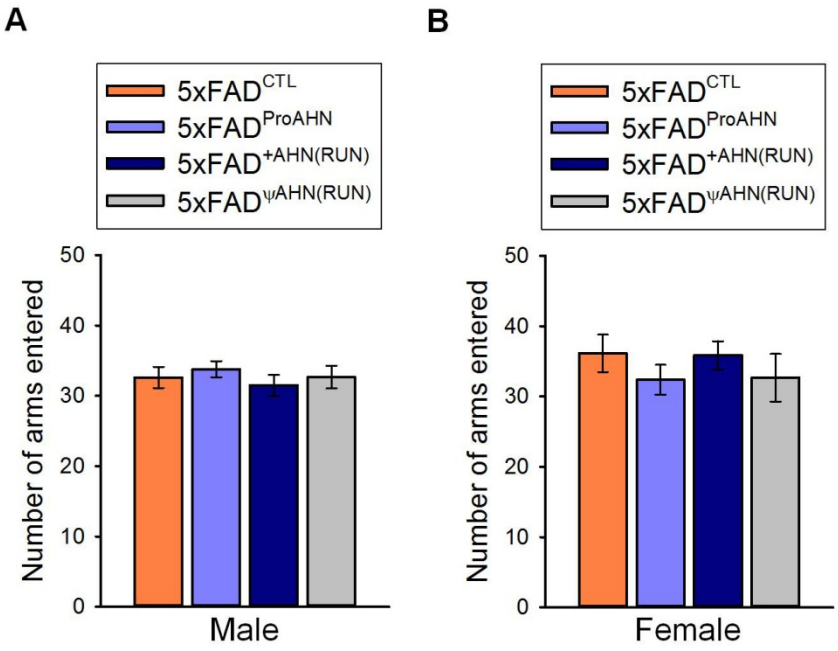

Fig. S4
Total number of arms entered during the Y-maze task.
(**A**, **B**) The total number of arms entered during the Y-maze task was comparable among 5×FAD^{CTL}, 5×FAD^{ProAHN}, 5×FAD$^{+AHN(RUN)}$, and 5×FAD$^{\psi AHN(RUN)}$ mice in each gender (A, male; B, female). See Table S1 for number of animals per group.

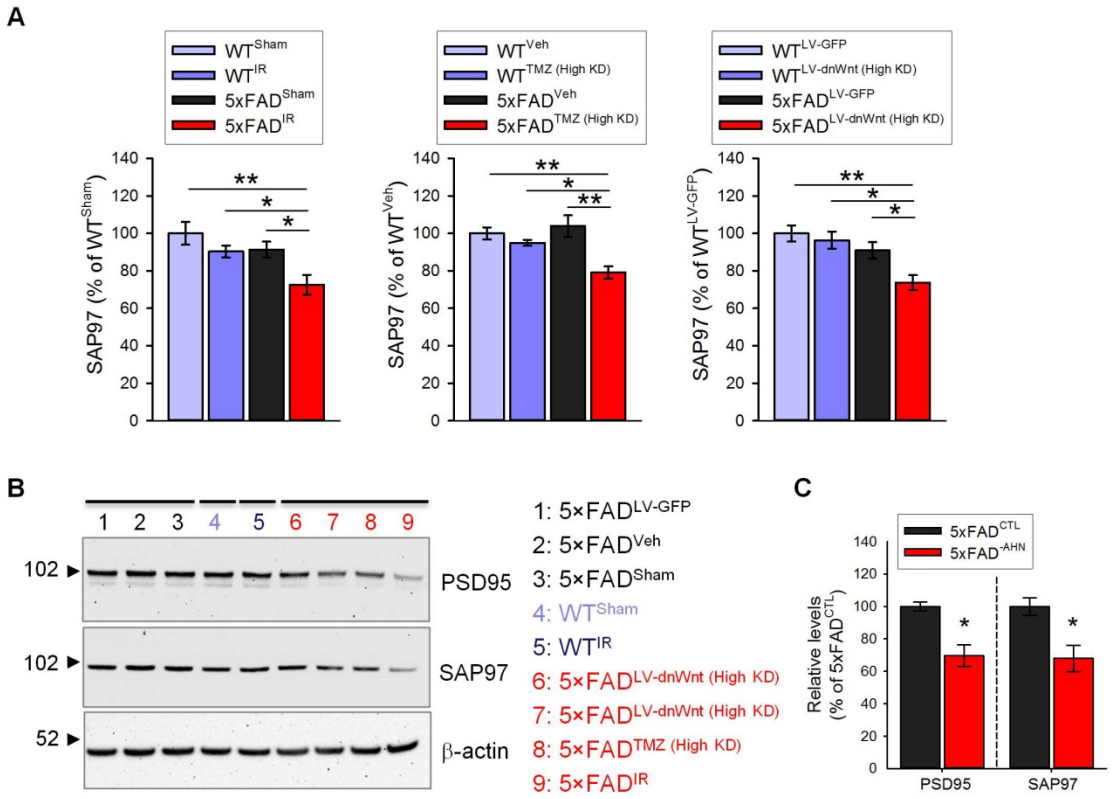

Fig. S5

Ablating AHN reduces hippocampal levels of synapse-associated protein 97 (SAP97) and PSD95 in 5×FAD mice.

(**A**) Levels of hippocampal SAP97 in WT^{Sham}, WT^{IR}, $5\times FAD^{Sham}$, and $5\times FAD^{IR}$ mice ($F_{(3,32)} = 5.945$, $P < 0.01$, left graph), in WT^{Veh}, $WT^{TMZ\ (High\ KD)}$, $5\times FAD^{Veh}$, and $5\times FAD^{TMZ\ (High\ KD)}$ mice ($F_{(3,33)} = 7.36$, $P < 0.01$, middle graph), and in $WT^{LV\text{-}GFP}$, $WT^{LV\text{-}dnWnt\ (High\ KD)}$, $5\times FAD^{LV\text{-}GFP}$, and $5\times FAD^{LV\text{-}dnWnt\ (High\ KD)}$ mice ($F_{(3,33)} = 6.275$, $P < 0.01$, right graph). *$P < 0.05$, **$P < 0.01$. See Table S2 for number of animals per group. (**B**) Immunoblot analysis of PSD95 and SAP97 in hippocampal homogenates of mice with or without AHN. This cohort of mice was not included in the cognitive testing. (**C**) Densitometry quantification of immunoblot results. *$P < 0.05$ between $5\times FAD^{CTL}$ ($5\times FAD$ mice with AHN in Fig. S5B) and $5\times FAD^{-AHN}$ ($5\times FAD$ mice without AHN in Fig. S5B) mice.

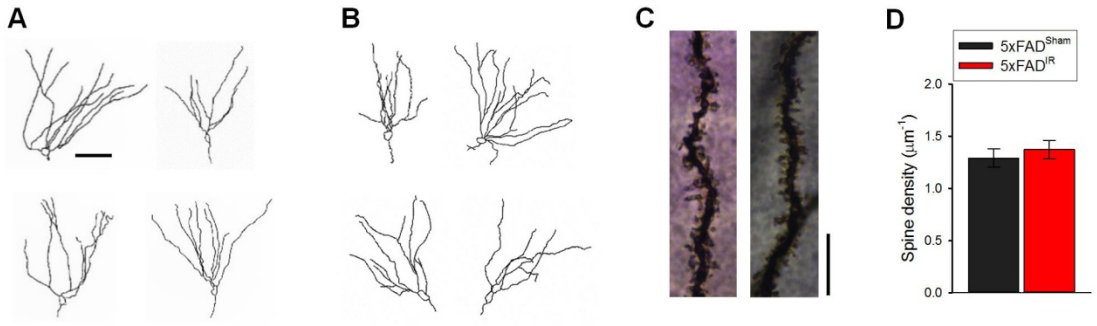

Fig. S6

Morphology of neurons in the outer granule cell layer using Golgi staining.

(**A**, **B**) Representative images of neurons in the outer granule cell layer of 5×FAD^{Sham} (A) and 5×FAD^{IR} (B) mice. Scale bar: 100 μm. (**C**) Representative high-magnification segments of dendrites from neurons in the outer granule cell layer of 5×FAD^{Sham} (left) and 5×FAD^{IR} (right) mice. Scale bar: 10 μm. (**D**) Quantification of spine density of neurons in the outer granule cell layer showed no difference between 5×FAD^{Sham} (n = 3) and 5×FAD^{IR} mice (n = 4). 7 neurons per mouse were examined. (**A-D**) This cohort of mice was not included in the cognitive testing.

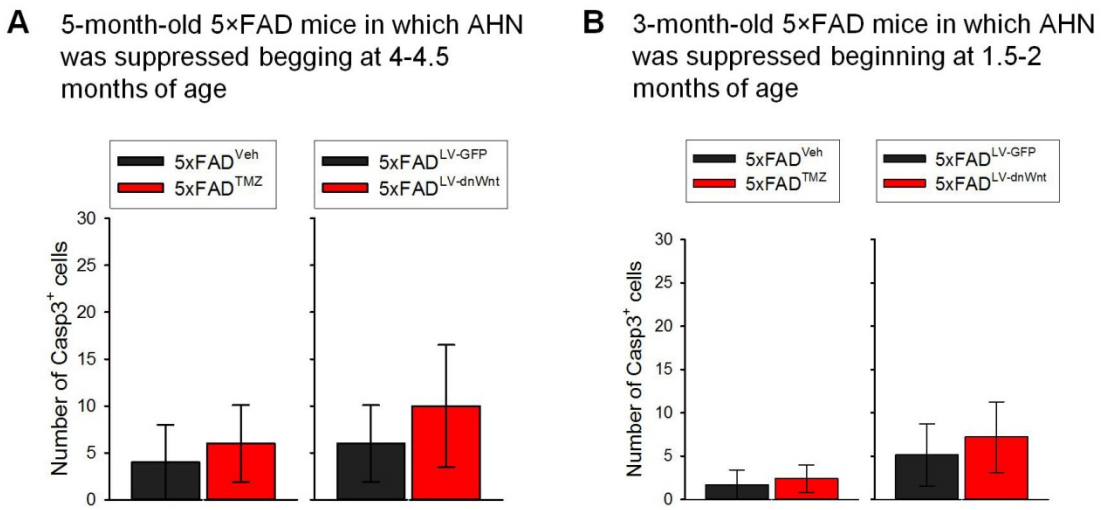

Fig. S7

AHN ablation starting at 4-4.5 months of age in 5×FAD mice does not induce cell death in the DG at 5 months of age, and ablation starting at 6 weeks of age in 5×FAD mice does not induce cell death in the DG at 3 months of age.

(**A**) Quantification of $Casp3^+$ cells in the DG of 5-month-old 5×FAD mice in which AHN was suppressed beginning at 4-4.5 months of age by TMZ or LV-dnWnt (n = 6 per group). (**B**) Quantification of $Casp3^+$ cells in the DG of 3-month-old 5×FAD mice in which AHN was suppressed beginning at 1.5-2 months of age of age by TMZ or LV-dnWnt (n = 7 in $5\times FAD^{Veh}$, 10 in $5\times FAD^{TMZ}$, 7 in $5\times FAD^{LV\text{-}GFP}$, and 10 in $5\times FAD^{LV\text{-}dnWnt}$ mice). (**A**, **B**) Irradiation was not used for these assays since it requires approximately 1 month recovery period.

A

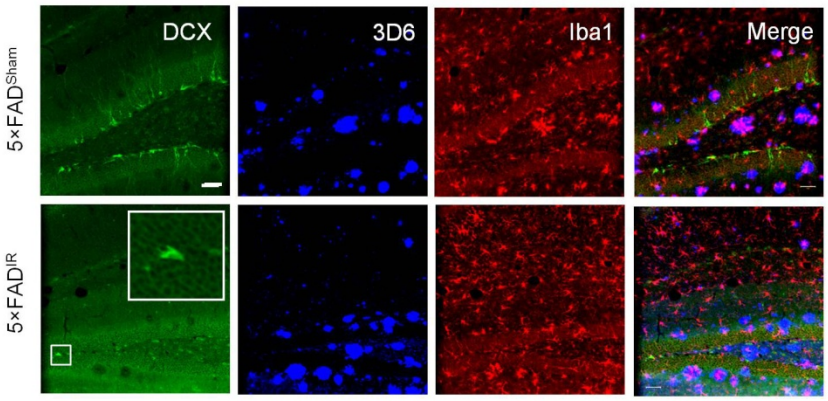

B

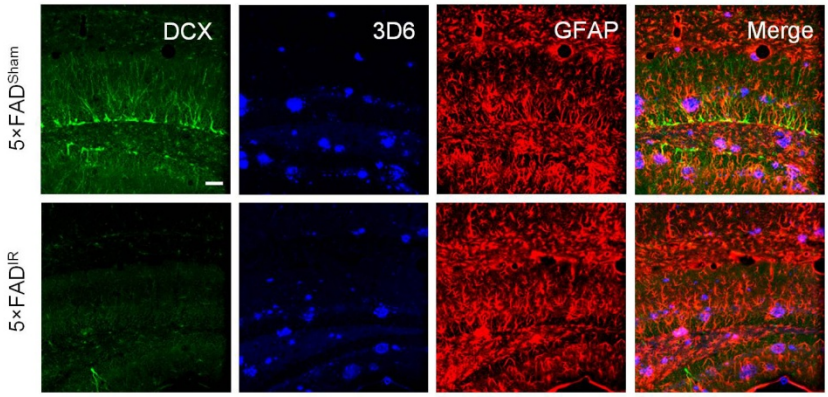

C

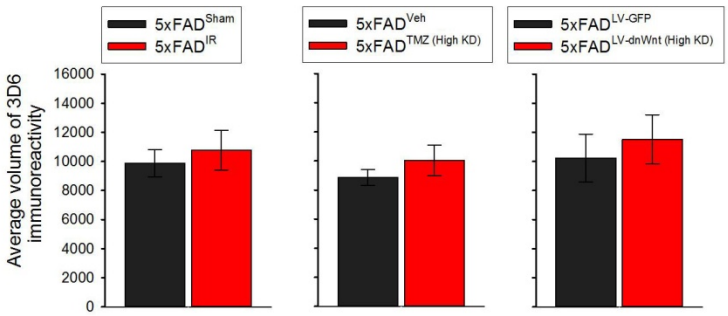

D

	Number of Iba1⁺ microglia in (200 μm)² (DG)	Number of GFAP⁺ astrocytes in (200 μm)² (DG)
5×FAD^{Sham}	14.929 ± 0.631	38.786 ± 2.138
5×FAD^{IR}	16.143 ± 0.762	39.357 ± 1.357
5×FAD^{Veh}	15.429 ± 0.702	39.357 ± 1.999
5×FAD$^{TMZ\ (High\ KD)}$	17.000 ± 0.939	40.500 ± 1.982
5×FAD$^{LV\text{-}GFP}$	17.643 ± 0.624	44.571 ± 1.329
5×FAD$^{LV\text{-}dnWnt\ (High\ KD)}$	18.071 ± 0.997	45.929 ± 2.048

Fig. S8

Ablating AHN does not affect Aβ pathology or gliosis.

(**A**, **B**) Confocal microscope images of DCX^+ neurons (green), $3D6^+$ Aβ plaques (blue), $Iba1^+$ microglia (red in A), and $GFAP^+$ astrocytes (red in B) in the DG of 5-month-old $5\times FAD^{Sham}$ (upper panels) and $5\times FAD^{IR}$ (lower panels) mice. The larger inset represents a digitally magnified image of the smaller outlined region for better visualization of DCX^+ neurons. Scale bars: 50 μm. (**C**) Quantitative analysis of the volume of amyloid burden in the hippocampus of 5-month-old $5\times FAD^{Sham}$ versus $5\times FAD^{IR}$ mice (left graph), $5\times FAD^{Veh}$ versus $5\times FAD^{TMZ\ (High\ KD)}$ mice (middle graph), or $5\times FAD^{LV\text{-}GFP}$ versus $5\times FAD^{LV\text{-}dnWnt\ (High\ KD)}$ mice (right graph). Volume is in arbitrary units (mean voxel count ± SEM). Quantification of $3D6^+$ amyloid plaques showed no significant differences between $5\times FAD^{Sham}$ and $5\times FAD^{IR}$, $5\times FAD^{Veh}$ and $5\times FAD^{TMZ\ (High\ KD)}$, or $5\times FAD^{LV\text{-}GFP}$ and $5\times FAD^{LV\text{-}dnWnt\ (High\ KD)}$ mice in the hippocampus at the age of 5 months. Veh, Vehicle; High KD, High AHN Knockdown. See Table S2 for number of animals per each group. (**D**) Quantification of $Iba1^+$ microglia showed no significant differences between $5\times FAD^{Sham}$ and $5\times FAD^{IR}$, $5\times FAD^{Veh}$ and $5\times FAD^{TMZ\ (High\ KD)}$, or $5\times FAD^{LV\text{-}GFP}$ and $5\times FAD^{LV\text{-}dnWnt\ (High\ KD)}$ mice in the hippocampus at the age of 5 months. Quantification of $GFAP^+$ astrocytes also showed no significant differences in these groups at the same age.

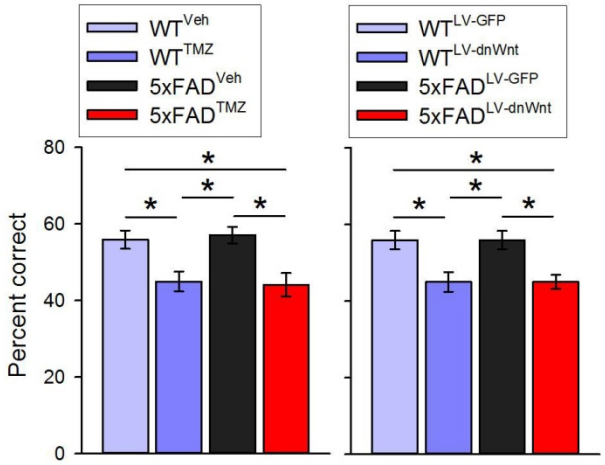

Fig. S9

Ablating AHN impairs pattern separation memory in 3-month-old WT and 5×FAD mice.

Quantification of percent correct during the choice phase of the DNMP task among 3-month-old WT^{Veh}, WT^{TMZ}, $5\times FAD^{Veh}$, and $5\times FAD^{TMZ}$ mice (n = 7 in WT^{Veh} and $5\times FAD^{Veh}$, 10 in WT^{TMZ} and $5\times FAD^{TMZ}$ mice; $F_{(3,30)} = 6.373$, $P < 0.01$, left graph), and among $WT^{LV\text{-}GFP}$, $WT^{LV\text{-}dnWnt}$, $5\times FAD^{LV\text{-}GFP}$, and $5\times FAD^{LV\text{-}dnWnt}$ mice (n = 7 in $WT^{LV\text{-}GFP}$ and $5\times FAD^{LV\text{-}GFP}$, 10 in $WT^{LV\text{-}dnWnt}$ and $5\times FAD^{LV\text{-}dnWnt}$ mice; $F_{(3,30)} = 7.215$, $P < 0.01$, right graph). *$P < 0.05$. Irradiation was not used for these assays since it requires approximately 1 month recovery period.

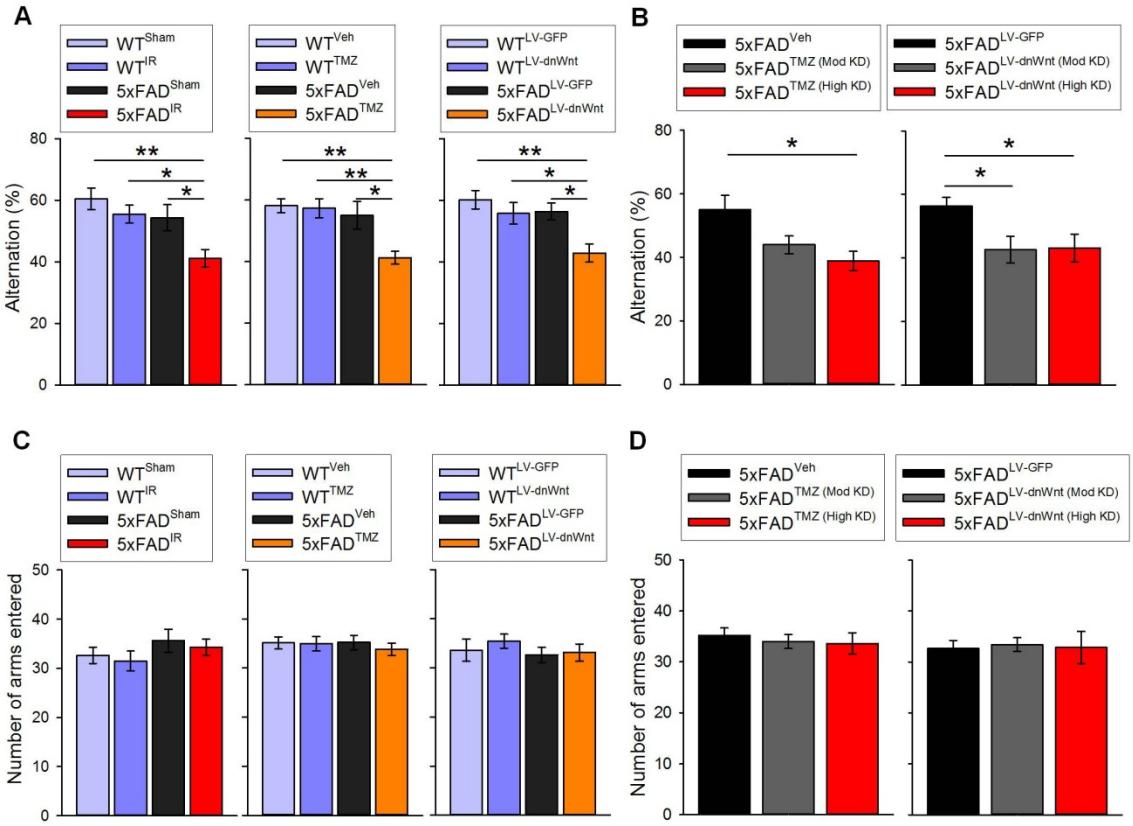

Fig. S10

Ablating AHN exacerbates the impairment of working memory in 5-month-old 5×FAD mice but not in WT mice.

(**A**) Spontaneous alternation behavior in the Y-maze task among WT^{Sham}, WT^{IR}, $5\times FAD^{Sham}$, and $5\times FAD^{IR}$ mice ($F_{(3,32)} = 6.37$, $P < 0.01$, left graph), among WT^{Veh}, WT^{TMZ}, $5\times FAD^{Veh}$, and $5\times FAD^{TMZ}$ mice ($F_{(3,46)} = 7.689$, $P < 0.01$, middle graph), and among $WT^{LV\text{-}GFP}$, $WT^{LV\text{-}dnWnt}$, $5\times FAD^{LV\text{-}GFP}$, and $5\times FAD^{LV\text{-}dnWnt}$ mice ($F_{(3,45)} = 6.533$, $P < 0.01$, right graph). *$P < 0.05$, **$P < 0.01$. See Table S2 for number of animals per each group. (**B**) Spontaneous alternation behavior in the Y-maze task among $5\times FAD^{Veh}$, $5\times FAD^{TMZ\ (Mod\ KD)}$, and $5\times FAD^{TMZ\ (High\ KD)}$ mice ($F_{(2,22)} = 5.05$, $P < 0.05$, left graph), and among $5\times FAD^{LV\text{-}GFP}$, $5\times FAD^{LV\text{-}dnWnt\ (Mod\ KD)}$, and $5\times FAD^{LV\text{-}dnWnt\ (High\ KD)}$ mice ($F_{(2,24)} = 5.156$, $P < 0.05$, right graph). *$P < 0.05$. (**C**) The total number of arms entered during the test was comparable among WT^{Sham}, WT^{IR}, $5\times FAD^{Sham}$, and $5\times FAD^{IR}$ mice (left graph), among WT^{Veh}, WT^{TMZ}, $5\times FAD^{Veh}$, and $5\times FAD^{TMZ}$ mice (middle graph), and among $WT^{LV\text{-}GFP}$, $WT^{LV\text{-}dnWnt}$, $5\times FAD^{LV\text{-}GFP}$, and $5\times FAD^{LV\text{-}dnWnt}$ mice (right graph). (**D**) The total number of arms entered during the test was comparable among $5\times FAD^{Veh}$, $5\times FAD^{TMZ\ (Mod\ KD)}$, and $5\times FAD^{TMZ\ (High\ KD)}$ mice (left graph), and among $5\times FAD^{LV\text{-}GFP}$, $5\times FAD^{LV\text{-}dnWnt\ (Mod\ KD)}$, and $5\times FAD^{LV\text{-}dnWnt\ (High\ KD)}$ mice (right graph).

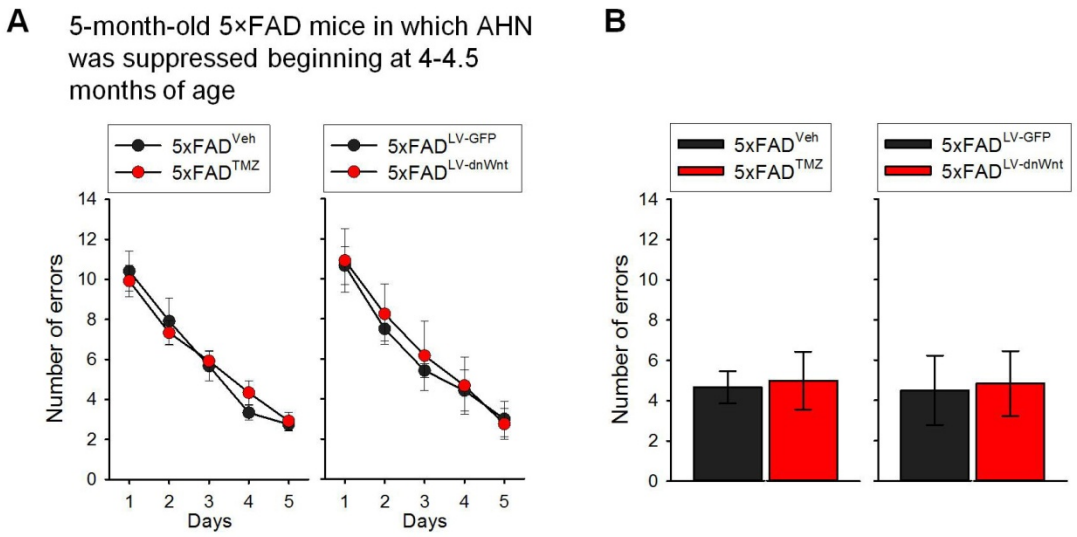

Fig. S11

Ablating AHN beginning at 4-4.5 months of age in 5×FAD mice does not exacerbate cognitive impairment at 5-months of age.

(**A**) Mean number of errors of 2 trials per day per group as a function of 5 consecutive training days in the RAM task between 5-month-old 5×FAD^{Veh} and 5×FAD^{TMZ} mice (left graph), and between 5×FAD$^{LV\text{-}GFP}$ and 5×FAD$^{LV\text{-}dnWnt}$ mice (right graph). Treatment began when mice were 4-4.5 months old (n = 6 per group). (**B**) Mean number of errors in the memory retention trial conducted 3 days after the last training trial in the reference memory test of RAM task between 5-month-old 5×FAD^{Veh} and 5×FAD^{TMZ} mice (left graph), and between 5×FAD$^{LV\text{-}GFP}$ and 5×FAD$^{LV\text{-}dnWnt}$ mice (right graph). (**A**, **B**) Irradiation was not used for these assays since it requires approximately 1 month recovery period.

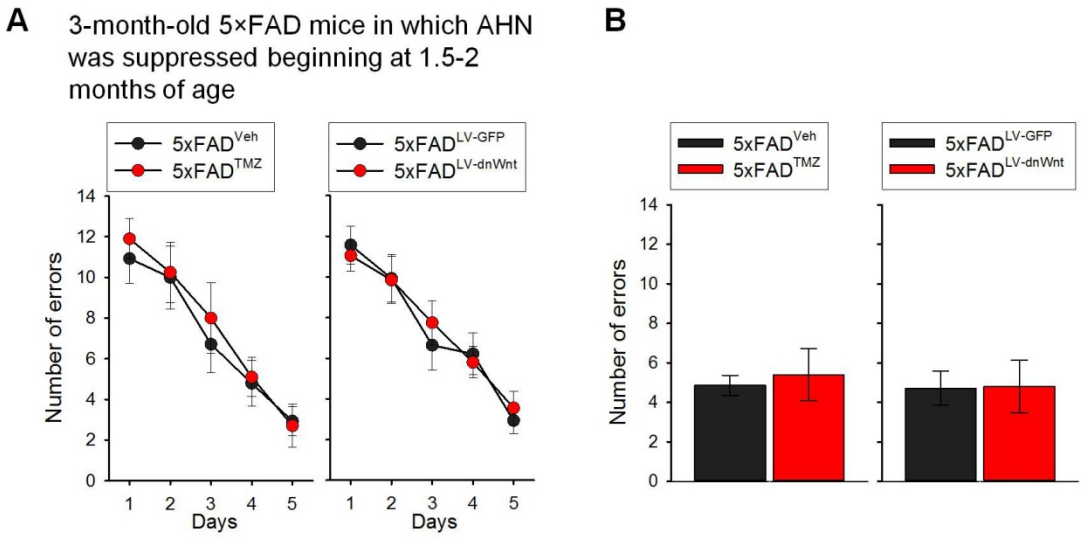

Fig. S12

Ablating AHN beginning at 6-8 weeks of age in 5×FAD mice does not exacerbate cognitive impairment at 3 months of age.

(**A**) Mean number of errors of 2 trials per day per group as a function of 5 consecutive training days in the RAM task between 3-month-old 5×FAD^{Veh} (n = 7) and 5×FAD^{TMZ} (n = 10) mice (left graph), and between 5×FAD$^{LV\text{-}GFP}$ (n = 7) and 5×FAD$^{LV\text{-}dnWnt}$ (n = 10) mice (right graph). (**B**) Mean number of errors in the memory retention trial conducted 3 days after the last training trial in the reference memory test of the RAM task between 3-month-old 5×FAD^{Veh} and 5×FAD^{TMZ} mice (left graph), and between 5×FAD$^{LV\text{-}GFP}$ and 5×FAD$^{LV\text{-}dnWnt}$ mice (right graph). (**A**, **B**) Irradiation was not used for these assays since it requires approximately 1 month recovery period.

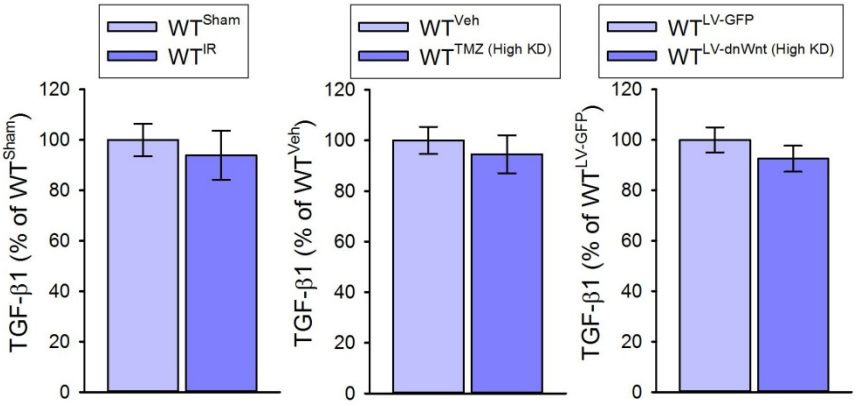

Fig. S13
Hippocampal TGF-β1 levels in WT mice with or without AHN.
Levels of hippocampal TGF-β1 in male WT^{Sham} and WT^{IR} (left), WT^{Veh} and $WT^{TMZ\ (High\ KD)}$ (middle), and $WT^{LV\text{-}GFP}$ and $WT^{LV\text{-}dnWnt\ (High\ KD)}$ mice (right). Levels as % of WT control group in each treatment.

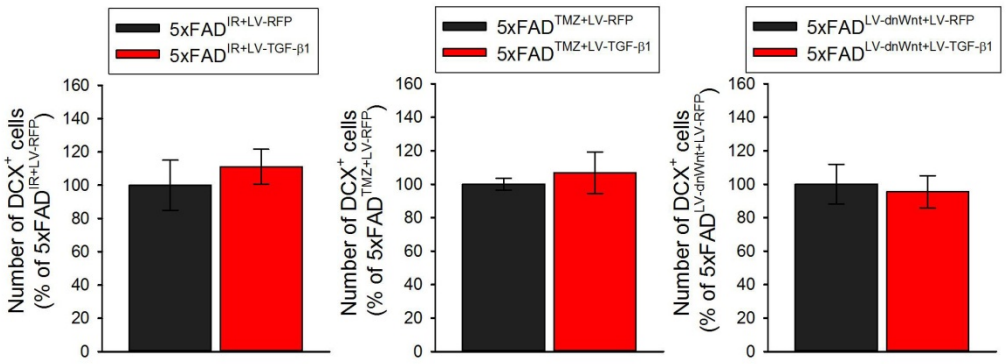

Fig. S14
Quantification of DCX$^+$ cells in 5×FAD^{-AHN} mice treated with LV-TGF-β1.
Number of DCX+ cells in 5×FAD$^{IR/LV-RFP}$ and 5×FAD$^{IR/LV-TGF-β1}$ (left), 5×FAD$^{TMZ/LV-RFP}$ and 5×FAD$^{TMZ/LV-TGF-β1}$ (middle), and 5×FAD$^{LV-dnWnt/LV-RFP}$ and 5×FAD$^{LV-dnWnt/LV-TGF-β1}$ (right) mice. Levels as % of 5×FAD control group in each treatment. Mice showed high or moderate AHN KD were used for this assay.

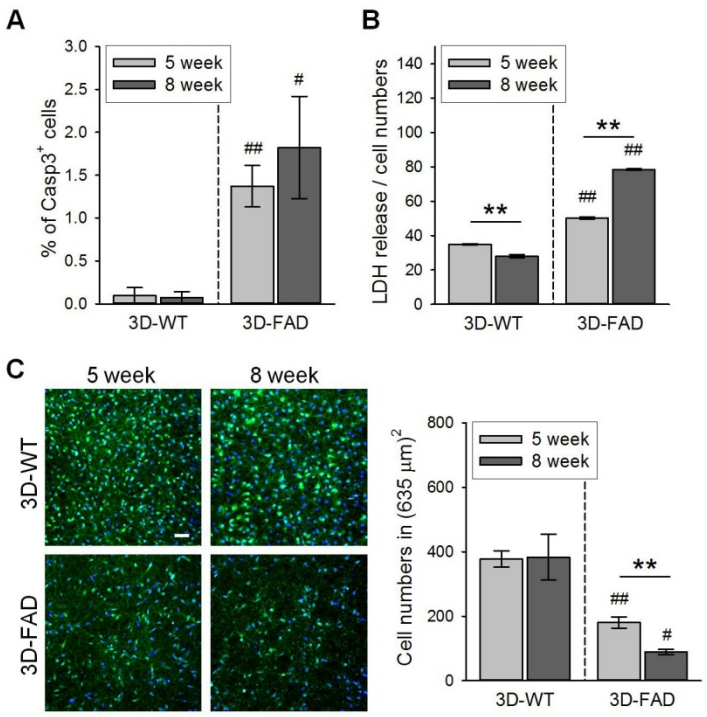

Fig. S15

Characterization of 3D-FAD cultures.

(**A**) The number of Casp3$^+$ cells in the 5- and 8-week differentiated 3D-WT and 3D-FAD cultures. The numbers of Casp3$^+$ cells in the 5- and 8-week differentiated 3D-FAD cultures were significantly higher compared to age-matched 3D-WT cultures. $^{\#}P < 0.05$, $^{\#\#}P < 0.01$ between 3D-FAD cultures and age-matched 3D-WT cultures. n = 4 per group. (**B**) Endogenous levels of LDH release detected in the media of 5- and 8-week differentiated 3D-WT and 3D-FAD cultures. The levels of LDH release were significantly higher in the 3D-FAD cultures compared to age-matched 3D-WT cultures. LDH release was also significantly higher in the 8-week differentiated 3D-FAD cultures compared to 5-week differentiated cultures. $^{**}P < 0.01$ between 5-week and 8-week differentiated 3D-FAD cultures and between 5-week and 8-week differentiated 3D-WT cultures. $^{\#\#}P < 0.01$ between 3D-FAD cultures and age-matched 3D-WT cultures. n = 4 per group. (**C**) Representative images of GFP-labeled 5- and 8-week differentiated 3D-WT and 3D-FAD cell cultures, and quantification of cells survived measured by number of DAPI$^+$ cells in these cultures. The number of cells was significantly lower in the 5- and 8-week differentiated 3D-FAD cultures compared to age-matched 3D-WT cultures. Additionally, a significantly lower number of cells was observed in the 8-week differentiated 3D-FAD cultures compared to 5-week differentiated 3D-FAD cultures. No difference was observed between 5- and 8-week differentiated 3D-WT cultures. Blue, DAPI. Scale bar: 50 μm. $^{**}P < 0.01$ between 5-week and 8-week differentiated 3D-FAD cultures. $^{\#}P < 0.05$, $^{\#\#}P < 0.01$ between 3D-FAD cultures and age-matched 3D-WT cultures. n = 4 per group. Altogether, the results of the Casp3$^+$ cell count (A), LDH release (B), and cell number (C) suggest that 3D-FAD cultures exhibit endogenous cell loss compared to 3D-WT cell cultures.

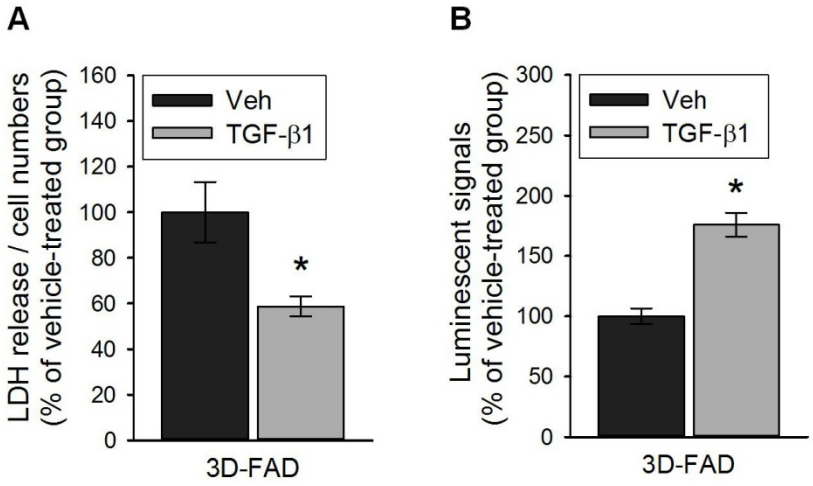

Fig. S16

Protective effects of TGF-β1 on cell death in 3D-FAD cultures

(**A**) LDH assay of 3D-FAD cell culture media treated for 2 weeks with either vehicle or TGF-β1 (10 ng/ml; *P < 0.05; n = 3 per group, performed in triplicate). (**B**) Levels of cell viability using CellTiter-Glo reagents, expressed as luminescent signals, in 3D-FAD cell cultures treated for 2 weeks with either vehicle or TGF-β1 (10 ng/ml; *P < 0.05; n = 4 per group, performed in triplicate).

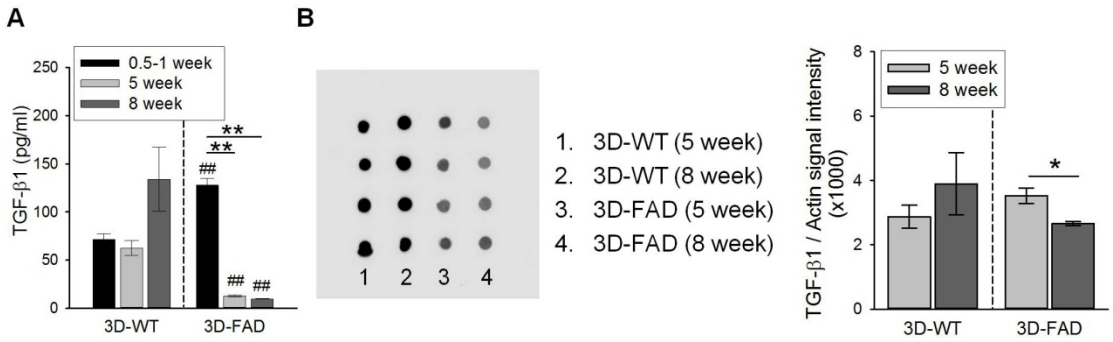

Fig. S17

Endogenous levels of TGF-β1 in the media of 3D-WT and 3D-FAD cultures

(**A**) Endogenous levels of TGF-β1 in the media of 0.5-, 5-, and 8-week differentiated 3D-WT and 3D-FAD cultures (in 3D-FAD, $F_{(2,14)} = 129.9$, $P < 0.01$; $^{**}P < 0.01$ between 0.5-1 week-differentiated 3D-FAD and 5- or 8 week-differentiated 3D-FAD cultures, $^{\#\#}P < 0.01$ between 3D-FAD and age-matched 3D-WT cultures, n = 4). (**B**) Actin signal intensity of 5- and 8-week differentiated 3D-WT and 3D-FAD cell cultures in dot-blot analysis, and endogenous levels of TGF-β1 in the media of 5- and 8-week differentiated 3D-WT and 3D-FAD cultures, normalized by actin signal density. This assay shows that TGF-β1 levels were not different between 3D-FAD cultures and age-matched 3D-WT cultures, suggesting that reduced TGF-β1 levels observed in 3D-FAD cultures compared to 3D-WT cultures are due to cell loss in this culture. However, we also observed that the levels of TGF-β1 that were normalized by actin signal density were significantly reduced in the 8-week differentiated 3D-FAD cultures compared to 5 week-differentiated 3D-FAD cultures ($^{*}P < 0.05$). Therefore, we cannot exclude the possibility that the reduced TGF-β1 level observed in 8-week differentiated 3D-FAD cultures are also attributed to specific signaling inhibitions.

A

Female	N		Analysis
5×FAD^{CTL}	8 2 in 5×FAD^{Sham} 3 in 5×FAD^{Veh} 3 in 5×FAD$^{LV\text{-}GFP}$		RAM and Y-maze tasks, DCX^{+} cell count, Casp3^{+} cell count, Levels of PSD95 and TGF-β1
5×FAD^{-AHN}	15 2 in 5×FAD^{IR} 7 in 5×FAD^{TMZ} 6 in 5×FAD$^{LV\text{-}dnWnt}$	6 in 5×FAD$^{-AHN\ (Mod\ KD)}$ 0 in 5×FAD^{IR} 3 in 5×FAD^{TMZ} 3 in 5×FAD$^{LV\text{-}dnWnt}$	
		9 in 5×FAD$^{-AHN\ (High\ KD)}$ 2 in 5×FAD^{IR} 4 in 5×FAD^{TMZ} 3 in 5×FAD$^{LV\text{-}dnWnt}$	

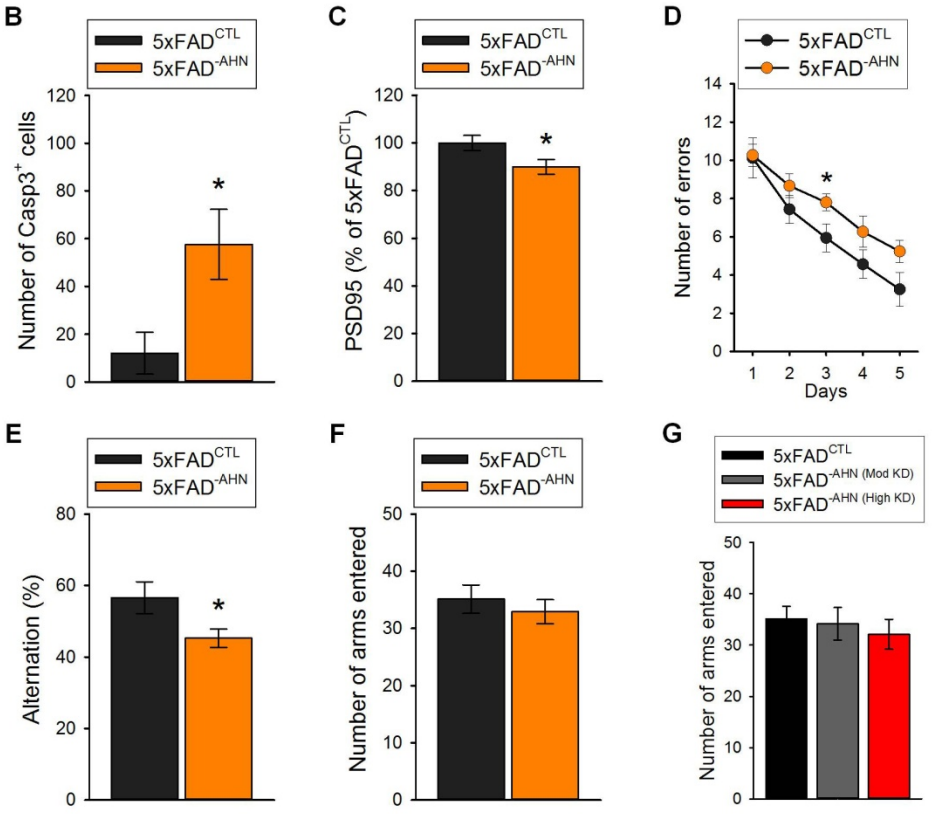

Fig. S18

The number of animals in each experimental group shown in Fig. 6A-6F, and results of Casp3^{+} cell counts, levels of hippocampal PSD95 measurement, RAM and Y-maze tasks in female 5×FAD mice with or without AHN.

(**A**) In the female cohorts, 8 5×FAD^{CTL} and 15 5×FAD^{-AHN} mice were used for the experiments listed in the table. The 5×FAD^{CTL} group included 2 5×FAD^{Sham}, 3 5×FAD^{Veh}, and 3 5×FAD$^{LV\text{-}GFP}$ mice. The 5×FAD^{-AHN} group included 2 5×FAD^{IR}, 7 5×FAD^{TMZ}, and 6 5×FAD$^{LV\text{-}dnWnt}$ mice. Out of the 15 5×FAD^{-AHN} mice, 6 mice showed moderate AHN knockdown (5×FAD$^{-AHN\ (Mod\ KD)}$ mice) and 9 mice showed high AHN

knockdown (5×FAD$^{-AHN\ (High\ KD)}$ mice). The 5×FAD$^{-AHN\ (Mod\ KD)}$ group included 3 5×FAD^{TMZ} and 3 5×FAD$^{LV\text{-}dnWnt}$ mice, and the 5×FAD$^{-AHN\ (High\ KD)}$ group included 2 5×FAD^{IR}, 4 5×FAD^{TMZ}, and 3 5×FAD$^{LV\text{-}dnWnt}$ mice. (**B**) Quantification of Casp3^{+} cells in the DG of 5-month-old female 5×FAD^{CTL} and 5×FAD^{-AHN} mice. The number of Casp3^{+} cells was significantly higher in 5×FAD^{-AHN} mice compared to 5×FAD^{CTL} mice (*$P < 0.05$). (**C**) Levels of PSD95 in the hippocampal homogenates of 5×FAD^{CTL} and 5×FAD^{-AHN} mice. Hippocampal level of PSD95 was significantly lower in 5×FAD^{-AHN} mice compared to 5×FAD^{CTL} mice (*$P < 0.05$). (**D**) Mean number of errors of 2 trials per day per group as a function of 5 consecutive training days in the RAM task between female 5×FAD^{CTL} and 5×FAD^{-AHN} mice. A significant difference in the number of errors was observed on day 3 between these two groups (*$P < 0.05$). (**E**, **F**) Spontaneous alternation behavior of 5×FAD^{CTL} and 5×FAD^{-AHN} mice during an 8-min session in the Y-maze task. Spontaneous alternation was impaired in 5×FAD^{-AHN} mice compared to 5×FAD^{CTL} mice (*$P < 0.05$) (E). The total number of arms entered during the test was comparable in these two groups (F). (**G**) Total number of arms entered in the Y-maze task by female 5×FAD^{CTL}, 5×FAD$^{-AHN\ (Mod\ KD)}$, and 5×FAD$^{-AHN\ (High\ KD)}$ mice. The total number of arms entered in the Y-maze task was comparable among these mice.

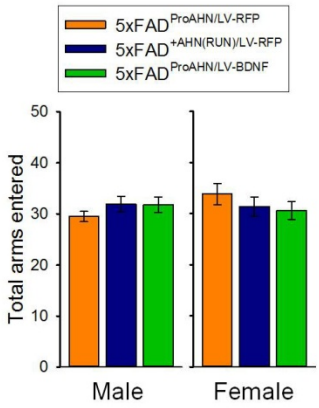

Fig. S19
Total number of arms entered in the Y-maze task by 5×FAD$^{ProAHN/LV-RFP}$, 5×FAD$^{+AHN/LV-RFP}$, and 5×FAD$^{ProAHN/LV-BDNF}$ mice.
The total number of arms entered in the Y-maze task was comparable among the three groups in each respective gender (male, left graph; female, right graph).

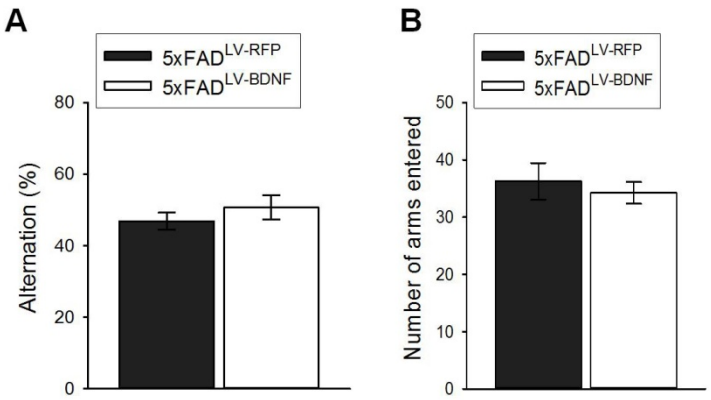

Fig. S20
Increase in BDNF alone by LV-BDNF does not ameliorate cognitive defects in 6-month old 5×FAD mice.
(**A**) Increasing BDNF alone, in the absence of promoting AHN by P7C3 and LV-Wnt3, failed to improve spontaneous alternation measured in the Y-maze task in 5×FAD mice (n = 8 in 5×FAD$^{LV\text{-}RFP}$ and 12 in 5×FAD$^{LV\text{-}BDNF}$ mice. (**B**) The total number of arms entered in the Y-maze task was comparable between 5×FAD$^{LV\text{-}RFP}$ and 5×FAD$^{LV\text{-}BDNF}$ mice.

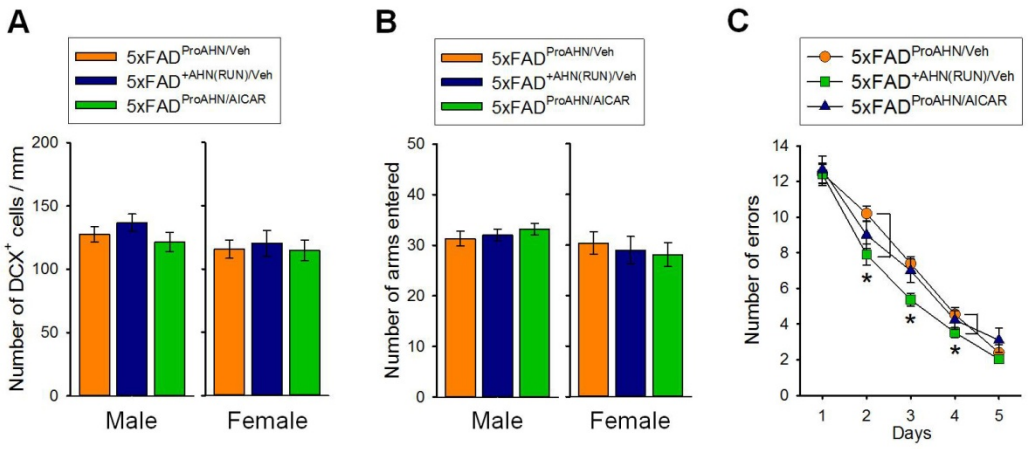

Fig. S21
Quantification of DCX$^+$ cells, total number of arms entered during the Y-maze task, and number of errors in the training trials in the RAM task among 5×FAD$^{ProAHN/Veh}$, 5×FAD$^{+AHN(RUN)/Veh}$, and 5×FAD$^{ProAHN/AICAR}$ mice.
(**A**) Quantification of DCX$^+$ cells among 5×FAD$^{ProAHN/Veh}$, 5×FAD$^{+AHN(RUN)/Veh}$, and 5×FAD$^{+AHN/AICAR}$ mice (male, left graph; female, right graph). No difference was observed among the three groups in each respective gender. (**B**) The total number of arms entered in the Y-maze task was comparable among the three groups in each respective gender. (**C**) Mean number of errors of 2 trials per day for the groups (male 5×FAD$^{ProAHN/Veh}$, 5×FAD$^{+AHN(RUN)/Veh}$, and 5×FAD$^{ProAHN/AICAR}$) as a function of 5 consecutive training days in the RAM task. A 2-way repeated measures ANOVA revealed significant effects for days ($F_{(4,188)} = 200.7$, $P < 0.01$) but not for groups ($F_{(3,47)} = 1.699$, $P = 0.180$) and interaction ($F_{(12,188)} = 0.952$, $P = 0.497$). Analysis of the number of errors on each day by Fisher's LSD post hoc tests exhibited a significant difference between 5×FAD$^{ProAHN/Veh}$ and 5×FAD$^{+AHN(RUN)/Veh}$ on days 2 and 4, and between 5×FAD$^{+AHN(RUN)/Veh}$ and the other two groups on day 3 (*$P < 0.05$). 5×FAD$^{ProAHN/AICAR}$ mice did not perform better than 5×FAD$^{ProAHN/Veh}$ mice in the training trials of the RAM task.

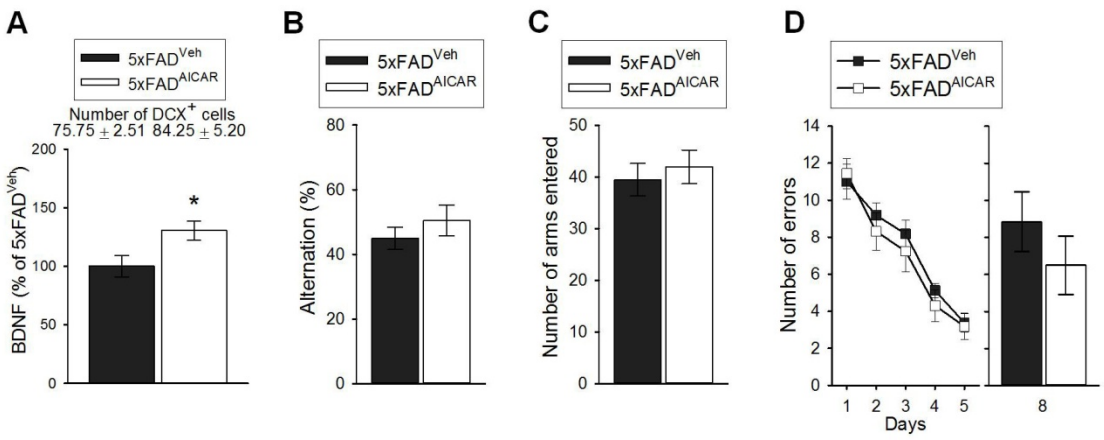

Fig. S22
Late-stage increase in BDNF alone by AICAR does not ameliorate cognitive defects in 6-month-old 5×FAD mice.
(**A**) Levels of hippocampal BDNF in 5×FAD^{Veh} and 5×FAD^{AICAR} mice (n = 8 per group). *P < 0.05. Number of DCX^{+} cells is listed above the graph. (**B**, **C**) Spontaneous alternation behavior (B) and the total number of arms entered (C) in the Y-maze task. (**D**) Left graph: Mean number of errors of 2 trials per day for the groups of 5×FAD^{Veh} and 5×FAD^{AICAR} as a function of 5 consecutive training days in the RAM task. Right graph: Mean number of errors in the memory retention trial of RAM task for 5×FAD^{Veh} and 5×FAD^{AICAR} mice.

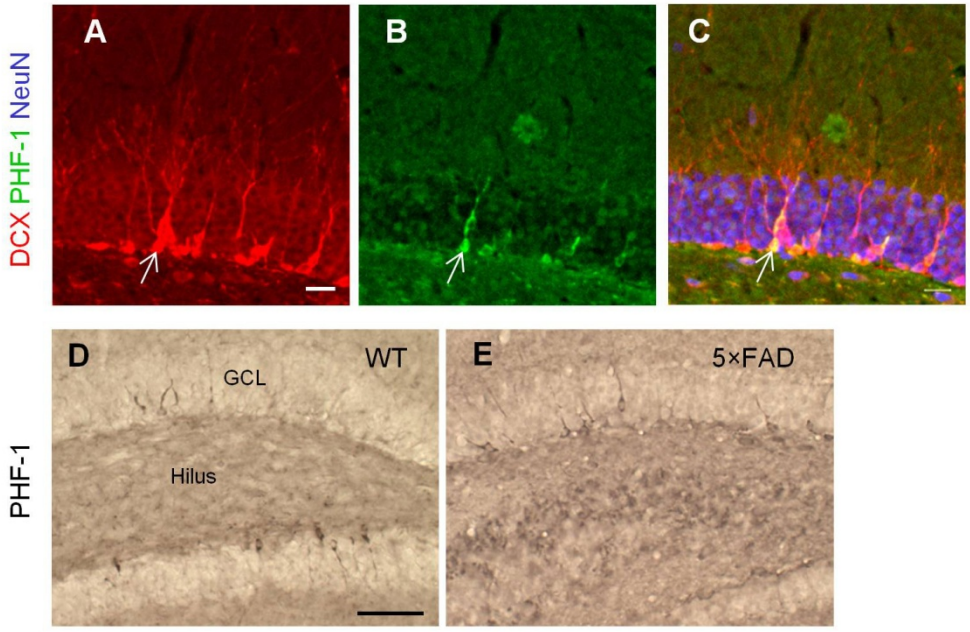

Fig. S23
Representative images of DCX$^+$/PHF-1$^+$ cells.
(**A**-**C**) Fractions of DCX$^+$ immature neurons were immunoreactive to the PHF-1 antibody, which recognizes tau proteins phosphorylated at serine residues 396 and 404 (pSer396/Ser404). Confocal images of DCX$^+$/PHF-1$^+$ neurons. Red, DCX$^+$ cells (A); Green, PHF-1$^+$ cells (B). Merged image is shown in (C). Blue, NeuN$^+$ cells. Arrows indicate the position of DCX$^+$PHF-1$^+$ neurons. Scale bar: 10 μm. (**D**-**E**) Photomicrographs of PHF-1$^+$ cells in the DG of WT (D) and 5×FAD (E) mice. GCL, granule cell layer. These cells are most likely adult-born neurons, rather than those undergoing tauopathy. Scale bar: 100 μm.

Male	5×FAD^{CTL}	5×FAD^{ProAHN}	5×FAD^{RUN}	
RAM task, DCX$^+$ cell count	10	19	23	
Mice used for further analysis: RAM task, Aβ pathology, PSD95, SYP, IL-6	**10**	**15** 4 mice that showed similar numbers of DCX$^+$ cells as those of 5×FAD^{CTL} were excluded.	5×FAD$^{+AHN(RUN)}$ **12** 3 mice that showed higher numbers of DCX$^+$ cells compared to the maximum number seen in 5×FAD^{ProAHN} were excluded.	5×FAD$^{ψAHN(RUN)}$ **8**
Y-maze, DNMP, DCX$^+$ cell count	8	14	19	
Mice used for further analysis: Y-maze, DNMP, Aβ pathology, BDNF, FNDC5, TGF-β1	**8**	**10** 4 mice that showed similar numbers of DCX$^+$ cells as those of 5×FAD^{CTL} were excluded.	5×FAD$^{+AHN(RUN)}$ **8** 2 mice that showed higher numbers of DCX$^+$ cells compared to the maximum number seen in 5×FAD^{ProAHN} were excluded.	5×FAD$^{ψAHN(RUN)}$ **9**

Female	5×FAD^{CTL}	5×FAD^{ProAHN}	5×FAD^{RUN}	
Y-maze, DNMP, DCX$^+$ cell count	7	10	13	
Mice used for further analysis: Y-maze, DNMP, Aβ pathology, BDNF, PSD95, IL-6, FNDC5	**7**	**8** 2 mice that showed similar numbers of DCX$^+$ cells as those of 5×FAD^{CTL} were excluded.	5×FAD$^{+AHN(RUN)}$ **7** 3 mice that showed higher numbers of DCX$^+$ cells compared to the maximum number seen in 5×FAD^{ProAHN} were excluded.	5×FAD$^{ψAHN(RUN)}$ **0** N = 3 data was excluded from further analysis due to this low N.

Table S1

The number of animals in each experimental group shown in Fig. 1 and 2.

In the male cohorts, 10 5×FAD^{CTL}, 19 5×FAD^{ProAHN}, and 23 5×FAD^{RUN} mice were tested in the RAM task, and the number of DCX$^+$ cells in the DG of these mice was counted. Among them, 10 5×FAD^{CTL}, 15 5×FAD^{ProAHN}, 12 5×FAD$^{+AHN(RUN)}$, and 8 5×FAD$^{ψAHN(RUN)}$ mice were used for statistical analysis of performance in the RAM task and for the experiments listed in the table. In a different cohort of male mice, 8 5×FAD^{CTL}, 14 5×FAD^{ProAHN}, and 19 5×FAD^{RUN} mice were tested in the Y-maze and DNMP tasks, and the number of DCX$^+$ cells in the DG of these mice was counted. Among them, 8 5×FAD^{CTL}, 10 5×FAD^{ProAHN}, 8 5×FAD$^{+AHN(RUN)}$, and 9 5×FAD$^{ψAHN(RUN)}$ mice were used for statistical analysis of performance in the Y-maze and DNMP tasks and for the experiments listed in the table. In the female cohorts, 7 5×FAD^{CTL}, 10 5×FAD^{ProAHN}, and 13 5×FAD^{RUN} mice were tested in the Y-maze and DNMP tasks, and the number of DCX$^+$ cells in the DG of these mice was counted. Among them, 7 5×FAD^{CTL}, 8 5×FAD^{ProAHN}, and 7 5×FAD$^{+AHN(RUN)}$ mice were used for statistical analysis of performance in the Y-maze and DNMP tasks and for the experiments listed in the table. The number of animals in female 5×FAD$^{ψAHN(RUN)}$ group was 3 and data from this group was excluded from analysis and further experiments due to the low n.

Male	N	Analysis
WT^{Sham}	10	RAM and Y-maze tasks, DCX^+ cell count, Aβ pathology, Gliosis, $Casp3^+$ cell count, Granule cell number, Levels of PSD95, SAP97, 10 cytokines (see table legend for cytokine list), and TGF-β1
WT^{IR}	12	
$5×FAD^{Sham}$	12	
$5×FAD^{IR}$	15	

Male	N		Analysis
WT^{Veh}	10		RAM and Y-maze tasks, DCX^+ cell count, $Casp3^+$ cell count, Aβ pathology, Gliosis, Granule cell number, Levels of PSD95, SAP97, 10 cytokines, and TGF-β1
WT^{TMZ}	15	Moderate AHN KD: 6	RAM and Y-maze tasks, DCX^+ cell count, $Casp3^+$ cell count
		High AHN KD: 9	RAM and Y-maze tasks, DCX^+ cell count, $Casp3^+$ cell count, Aβ pathology, Gliosis, Granule cell number, Levels of PSD95, SAP97, 10 cytokines, and TGF-β1
$5×FAD^{Veh}$	10		RAM and Y-maze tasks, DCX^+ cell count, $Casp3^+$ cell count, Aβ pathology, Gliosis, Granule cell number, Levels of PSD95, SAP97, 10 cytokines, and TGF-β1
$5×FAD^{TMZ}$	15	Moderate AHN KD: 7	RAM and Y-maze tasks, DCX^+ cell count, $Casp3^+$ cell count
		High AHN KD: 8	RAM and Y-maze tasks, DCX^+ cell count, $Casp3^+$ cell count, Aβ pathology, Gliosis, Granule cell number, Levels of PSD95, SAP97, 10 cytokines, and TGF-β1

Male	N		Analysis
$WT^{LV\text{-}GFP}$	10		RAM and Y-maze tasks, DCX^+ cell count, $Casp3^+$ cell count, Aβ pathology, Gliosis, Granule cell number, Levels of PSD95, SAP97, 10 cytokines, and TGF-β1
$WT^{LV\text{-}dnWnt}$	12	Moderate AHN KD: 5	RAM and Y-maze tasks, DCX^+ cell count, $Casp3^+$ cell count
		High AHN KD: 7	RAM and Y-maze tasks, DCX^+ cell count, $Casp3^+$ cell count, Aβ pathology, Gliosis, Granule cell number, Levels of PSD95, SAP97, 10 cytokines, and TGF-β1
$5×FAD^{LV\text{-}GFP}$	12		RAM and Y-maze tasks, DCX^+ cell count, $Casp3^+$ cell count, Aβ pathology, Gliosis, Granule cell number, Levels of PSD95, SAP97, 10 cytokines, and TGF-β1
$5×FAD^{LV\text{-}dnWnt}$	15	Moderate AHN KD: 7	RAM and Y-maze tasks, DCX^+ cell count, $Casp3^+$ cell count
		High AHN KD: 8	RAM and Y-maze tasks, DCX^+ cell count, $Casp3^+$ cell count, Aβ pathology, Gliosis, Granule cell number, Levels of PSD95, SAP97, 10 cytokines, and TGF-β1

Table S2
The number of male animals in each experimental group shown in Fig. 3, 4B-4C, 4E-4F, S5, S8, S10, and S13.
10 WT^{Sham}, 12 WT^{IR}, 12 $5×FAD^{Sham}$, and 15 $5×FAD^{IR}$ mice were used for the experiments listed in the table. All 12 WT^{IR} and 15 $5×FAD^{IR}$ mice showed high AHN knockdown (KD). 10 WT^{Veh}, 15 WT^{TMZ}, 10 $5×FAD^{Veh}$, and 15 $5×FAD^{TMZ}$ mice were

tested in the RAM and Y-maze tasks, and the number of DCX^+ cells and $Casp3^+$ cells in the DG of these mice were counted. Out of 15 WT^{TMZ} mice, 6 mice showed moderate AHN KD and 9 mice showed high AHN KD. Out of 15 $5\times FAD^{TMZ}$ mice, 7 mice showed moderate AHN KD and 8 mice showed high AHN KD. Only the cohort of mice that showed high AHN KD and the vehicle-treated mice were used for the additional experiments listed in the table. 10 $WT^{LV\text{-}GFP}$, 12 $WT^{LV\text{-}dnWnt}$, 12 $5\times FAD^{LV\text{-}GFP}$, and 15 $5\times FAD^{LV\text{-}dnWnt}$ mice were tested in the RAM and Y-maze tasks, and the number of DCX^+ cells and $Casp3^+$ cells in the DG of these mice were counted. Out of 12 $WT^{LV\text{-}dnWnt}$ mice, 5 mice showed moderate AHN KD and 7 mice showed high AHN KD. Out of 15 $5\times FAD^{LV\text{-}dnWnt}$ mice, 7 mice showed moderate AHN KD and 8 mice showed high AHN KD. Only the cohort of mice that showed high AHN KD and vehicle-treated mice were used for the additional experiments listed in the table. The 10 cytokines measured include IFNγ, IL-1β, IL-2, IL-4, IL-5, IL-6, IL-10, IL-12p70, TNFα, and KC/GRO.

Left graphs: WT^{Sham} (n = 8), WT^{IR} (n = 10), $5\times FAD^{Sham}$ (n = 8), $5\times FAD^{IR}$ (n = 10)
A two-way ANOVA with repeated measures: Significant effects for days ($F_{(4,128)} = 91.47$, $p < 0.01$) and for groups ($F_{(3,32)} = 11.67$, $p < 0.01$), but not for interaction ($F_{(12,128)} = 0.998$, $p = 0.455$).
Fisher's LSD post hoc tests: A significant increase in the number of errors in $5\times FAD^{IR}$ mice when compared to all other groups on days 3-5. *P < 0.05; **P < 0.01.

Middle graphs: WT^{Veh} (n = 10), WT^{TMZ} (n = 15), $5\times FAD^{Veh}$ (n = 10), $5\times FAD^{TMZ}$ (n = 15)
A two-way ANOVA with repeated measures: Significant effects for days ($F_{(4,184)} = 221.8$, $p < 0.01$), for groups ($F_{(3,46)} = 18.21$, $p < 0.01$), and for interaction ($F_{(12,184)} = 2.684$, $p < 0.01$).
Fisher's LSD post hoc tests: A significant difference in the number of errors between $5\times FAD^{TMZ}$ and the following 2 groups, WT^{Veh} and WT^{TMZ} mice, on day 2; between $5\times FAD^{Veh}$ and the following 2 groups, WT^{Veh} and WT^{TMZ} mice, on day 2; between $5\times FAD^{TMZ}$ and all other groups on day 3 and day 5; between $5\times FAD^{TMZ}$ and the following 2 groups, WT^{Veh} and WT^{TMZ} mice, on day 4. *P < 0.05; **P < 0.01.

Right graphs: $WT^{LV\text{-}GFP}$ (n = 10), $WT^{LV\text{-}dnWnt}$ (n = 12), $5\times FAD^{LV\text{-}GFP}$ (n = 12), $5\times FAD^{LV\text{-}dnWnt}$ (n = 15)
A two-way ANOVA with repeated measures: Significant effects for days ($F_{(4,180)} = 124.2$, $p < 0.01$) and for groups ($F_{(3,45)} = 24.25$, $p < 0.01$), but not for interaction ($F_{(12,180)} = 1.494$, $p = 0.130$).
Fisher's LSD post hoc tests: A significant difference in the number of errors in $5\times FAD^{LV\text{-}dnWnt}$ when compared to all other groups on day 2, 4 and 5; in $5\times FAD^{LV\text{-}GFP}$ mice when compared to all other groups on day 2; in $5\times FAD^{LV\text{-}GFP}$ mice when compared to $WT^{LV\text{-}GFP}$ mice on day 3. *P < 0.05; **P < 0.01.

Table S3
Statistical analysis of performance in the RAM task of WT and 5×FAD mice with or without AHN (Fig. 4E).

Left graphs: $5\times FAD^{Veh}$ (n = 10), $5\times FAD^{TMZ\ (Mod\ KD)}$ (n = 7), $5\times FAD^{TMZ\ (High\ KD)}$ (n = 8)
A two-way ANOVA with repeated measures: Significant effects for days ($F_{(4,88)}$ = 80.81, p < 0.01), for groups ($F_{(2,22)}$ = 12.88, p < 0.01), but not for interaction ($F_{(8,88)}$ = 1.434, p = 0.1936).
Fisher's LSD post hoc tests: A significant difference in the number of errors between $5\times FAD^{TMZ\ (High\ KD)}$ and $5\times FAD^{Veh}$ mice on day 2 (*P < 0.05); between $5\times FAD^{TMZ\ (High\ KD)}$ and $5\times FAD^{Veh}$ mice on day 5 (**P < 0.01); between $5\times FAD^{TMZ\ (High\ KD)}$ and $5\times FAD^{TMZ\ (Mod\ KD)}$ mice on day 5 (*P < 0.05).

Right graphs: $5\times FAD^{LV\text{-}GFP}$ (n = 12), $5\times FAD^{LV\text{-}dnWnt\ (Mod\ KD)}$ (n = 7), $5\times FAD^{LV\text{-}dnWnt\ (High\ KD)}$ (n = 8)
A two-way ANOVA with repeated measures: Significant effects for days ($F_{(4,96)}$ = 51.75, p < 0.01) and for groups ($F_{(2,24)}$ = 17.69, p < 0.01), but not for interaction ($F_{(8,96)}$ = 0.6041, p = 0.7723).
Fisher's LSD post hoc tests: A significant difference in the number of errors between $5\times FAD^{LV\text{-}dnWnt\ (High\ KD)}$ and $5\times FAD^{LV\text{-}GFP}$ mice on day 4 (**P < 0.01); between $5\times FAD^{LV\text{-}dnWnt\ (High\ KD)}$ and $5\times FAD^{LV\text{-}GFP}$ mice on day 5 (**P < 0.01); between $5\times FAD^{LV\text{-}dnWnt\ (High\ KD)}$ and $5\times FAD^{LV\text{-}dnWnt\ (Mod\ KD)}$ mice on day 5 (*P < 0.05).

Table S4
Statistical analysis of the performance in the RAM task among $5\times FAD^{Veh}$, $5\times FAD^{TMZ\ (Mod\ KD)}$, and $5\times FAD^{TMZ\ (High\ KD)}$ mice, and among $5\times FAD^{LV\text{-}GFP}$, $5\times FAD^{LV\text{-}dnWnt\ (Mod\ KD)}$, and $5\times FAD^{LV\text{-}dnWnt\ (High\ KD)}$ mice (Fig. 4F).

.

Cytokines	5×FAD^{Sham}	5×FAD^{IR}
IFNγ	100.00 ± 7.73	90.97 ± 7.60
IL-1β	100.00 ± 3.90	88.45 ± 6.92
IL-2	100.00 ± 8.96	97.19 ± 8.91
IL-4	100.00 ± 9.16	93.75 ± 7.23
IL-5	100.00 ± 8.09	95.66 ± 10.88
IL-6	100.00 ± 5.99	107.71 ± 8.36
IL-10	100.00 ± 9.80	100.91 ± 7.13
IL-12p70	100.00 ± 14.48	107.64 ± 7.84
TNFα	100.00 ± 8.46	93.38 ± 11.90
KC/GRO	100.00 ± 6.36	112.09 ± 11.14

Cytokines	5×FAD^{Veh}	5×FAD$^{TMZ\ (High\ KD)}$
IFNγ	100.00 ± 7.33	89.48 ± 6.62
IL-1β	100.00 ± 5.91	105.77 ± 6.54
IL-2	100.00 ± 7.73	104.59 ± 6.70
IL-4	100.00 ± 7.14	94.64 ± 10.74
IL-5	100.00 ± 8.25	93.35 ± 8.97
IL-6	100.00 ± 6.75	102.52 ± 7.29
IL-10	100.00 ± 6.94	101.74 ± 6.47
IL-12p70	100.00 ± 6.22	104.81 ± 7.45
TNFα	100.00 ± 4.68	102.13 ± 16.12
KC/GRO	100.00 ± 7.37	123.07 ± 12.87

Cytokines	5×FAD$^{LV\text{-}GFP}$	5×FAD$^{LV\text{-}dnWnt\ (High\ KD)}$
IFNγ	100.00 ± 6.79	89.21 ± 7.32
IL-1β	100.00 ± 4.34	96.80 ± 6.48
IL-2	100.00 ± 8.45	106.40 ± 7.20
IL-4	100.00 ± 9.89	94.08 ± 12.62
IL-5	100.00 ± 7.57	95.94 ± 13.32
IL-6	100.00 ± 6.06	118.14 ± 12.97
IL-10	100.00 ± 6.20	101.68 ± 8.36
IL-12p70	100.00 ± 6.26	106.93 ± 6.35
TNFα	100.00 ± 9.68	93.76 ± 7.87
KC/GRO	100.00 ± 7.29	106.53 ± 13.81

Table S5

Ablating AHN does not change hippocampal levels of 10 cytokines in 5×FAD mice. Reducing AHN did not change the levels of 10 cytokines (IFNγ, IL-1β, IL-2, IL-4, IL-5, IL-6, IL-10, IL-12p70, TNFα, and KC/GRO) in the hippocampal homogenates of 5×FAD mice at the age of 5 months. Levels are presented as % of the 5×FAD control group in each treatment. See Table S2 for number of animals per group.

Molecules	Non-treated sedentary 5×FAD	Non-treated exercised 5×FAD
BDNF	100.00 ± 7.39	124.89 ± 8.14*
VEGF	100.00 ± 5.04	104.47 ± 6.94
NGF	100.00 ± 6.68	110.93 ± 6.17
IGF-1	100.00 ± 9.59	108.04 ± 14.18
FNDC5	100.00 ± 8.14	125.33 ± 7.79*
IFNγ	100.00 ± 7.47	103.41 ± 9.95
IL-1β	100.00 ± 4.53	87.97 ± 4.37 (P = 0.079)
IL-2	100.00 ± 7.24	105.03 ± 8.11
IL-4	100.00 ± 11.32	95.76 ± 10.19
IL-5	100.00 ± 9.20	99.35 ± 5.90
IL-6	100.00 ± 6.06	123.64 ± 8.29*
IL-10	100.00 ± 5.64	106.94 ± 7.19
IL-12p70	100.00 ± 7.09	90.47 ± 6.95
TNFα	100.00 ± 7.49	85.72 ± 5.75 (P = 0.149)
KC/GRO	100.00 ± 10.21	92.64 ± 7.02 (P = 0.554)
PSD95	100.00 ± 5.41	121.38 ± 6.97*
SYP	100.00 ± 5.05	119.10 ± 6.12*
Synapsin I	100.00 ± 6.74	115.88 ± 8.55

Table S6

The levels of BDNF, vascular endothelial growth factor (VEGF), nerve growth factor (NGF), insulin-like growth factor-1 (IGF-1), FNDC5, IFNγ, IL-1β, IL-2, IL-4, IL-5, IL-6, IL-10, IL-12p70, TNFα, KC/GRO, PSD95, SYP, and Synapsin I in non-treated sedentary and non-treated exercised 5×FAD mice.

The levels of BDNF, FNDC5, IL-6, PSD95, and SYP were significantly higher in the hippocampal homogenates of exercised 5×FAD mice compared to sedentary 5×FAD mice at 6 months of age (*P < 0.05, n = 7 or 8 per group). 5-month-old 5×FAD mice showed increased levels of IL-1β, TNFα, and KC/GRO compared to 3-month-old 5×FAD mice (Fig. S3). Exercise reduced the levels of IL-1β in 5×FAD mice, but it did not reach statistical significance (P = 0.079). Neither TNFα nor KC/GRO levels were changed by exercise in 5×FAD mice. Levels are presented as % of the sedentary 5×FAD group in each assay.

	5×FAD^{CTL}	5×FAD^{ProAHN}	5×FAD$^{+AHN(RUN)}$	5×FAD$^{ψAHN(RUN)}$
BDNF	100.00 ± 4.44 (7)	97.71 ± 6.21 (8)	121.52 ± 6.38* (7)	N=3. Data was excluded from further analysis due to the low N.
PSD95	100.00 ± 6.30 (7)	101.05 ± 4.30 (8)	130.16 ± 9.36* (7)	
IL-6	100.00 ± 3.53 (7)	97.62 ± 6.48 (8)	121.34 ± 5.90* (7)	
FNDC5	100.00 ± 5.80 (7)	104.60 ± 4.83 (8)	121.18 ± 7.86 (7)	

Table S7
Levels of hippocampal BDNF, PSD95, IL-6 and FNDC5 of female 5×FAD^{CTL}, 5×FAD^{ProAHN}, 5×FAD$^{+AHN(RUN)}$, and 5×FAD$^{ψAHN(RUN)}$ mice.
Number of animals is indicated in parentheses (also in Table S1). $F_{(2,19)} = 5.032$, $P < 0.05$ (BDNF); $F_{(2,19)} = 6.232$, $P < 0.01$ (PSD95); $F_{(2,19)} = 5.4$, $P < 0.05$ (IL-6); $F_{(2,19)} = 3.131$, $P = 0.07$ (FNDC5). *$P < 0.05$ compared to 5×FAD^{CTL} and 5×FAD^{ProAHN} mice. The number of animals in female 5×FAD$^{ψAHN(RUN)}$ group was 3 and data from this group was excluded due to the low n.

Groups	N	Fig. 7B	Fig. 7D	Fig. 7E	Fig. 7G
Male 5×FAD$^{ProAHN/LV-RFP}$	8	$F_{(2,35)} = 10.15$, $p < 0.01$	$F_{(2,35)} = 7.262$, $p < 0.01$	$F_{(2,35)} = 5.993$, $p < 0.01$	
Male 5×FAD$^{+AHN(RUN)/LV-RFP}$	15				
Male 5×FAD$^{ProAHN/LV-BDNF}$	15				
Female 5×FAD$^{ProAHN/LV-RFP}$	6	$F_{(2,27)} = 6.753$, $p < 0.01$	$F_{(2,27)} = 12.86$, $p < 0.01$	$F_{(2,27)} = 4.849$, $p < 0.05$	$F_{(2,27)} = 5.348$, $p < 0.05$
Female 5×FAD$^{+AHN(RUN)/LV-RFP}$	11				
Female 5×FAD$^{ProAHN/LV-BDNF}$	13				

Groups	N	Fig. 7F	
Male 5×FAD$^{ProAHN/LV-RFP}$	8	Left graph: A two-way ANOVA with repeated measures: Significant effects for days ($F_{(4,140)} = 114$, $p < 0.01$), groups ($F_{(2,35)} = 3.951$, $p = 0.0284$), but not for interaction ($F_{(8,140)} = 1.471$, $p = 0.1730$). Fisher's LSD post hoc tests: A significant difference in the number of errors between 5×FAD$^{ProAHN/LV-RFP}$ and 5×FAD$^{+AHN(RUN)/LV-RFP}$ mice, on day 2, 3, and 4. *P < 0.05; **P < 0.01.	Right graph: $F_{(2,35)} = 4.069$, $p < 0.05$
Male 5×FAD$^{+AHN(RUN)/LV-RFP}$	15		
Male 5×FAD$^{ProAHN/LV-BDNF}$	15		

Groups	N	Fig. 7J	Fig. 7K	Fig. 7L	Fig. 7M
Male 5×FAD$^{ProAHN/Veh}$	10	$F_{(2,37)} = 7.425$, $p < 0.01$	$F_{(2,37)} = 4.91$, $p < 0.05$	$F_{(2,37)} = 4.143$, $p < 0.05$	
Male 5×FAD$^{+AHN(RUN)/Veh}$	15				
Male 5×FAD$^{ProAHN/AICAR}$	15				
Female 5×FAD$^{ProAHN/Veh}$	8	$F_{(2,25)} = 5.031$, $p < 0.05$	$F_{(2,25)} = 5.223$, $p < 0.05$		$F_{(2,25)} = 5.668$, $p < 0.01$
Female 5×FAD$^{+AHN(RUN)/Veh}$	10				
Female 5×FAD$^{ProAHN/AICAR}$	10				

Table S8
Number of animals per group and statistical analysis of Fig. 7 experiments.

Male	PSD95	IL-6
5×FAD$^{ProAHN/LV-RFP}$ (8)	100.00 ± 2.56	100.00 ± 5.44
5×FAD$^{+AHN(RUN)/LV-RFP}$ (15)	127.63 ± 5.63**	125.16 ± 7.43*
5×FAD$^{ProAHN/LV-BDNF}$ (15)	119.72 ± 4.69*	96.83 ± 6.39
5×FAD^{LV-RFP} (8)	100.00 ± 7.17	100.00 ± 5.50
5×FAD$^{LV-BDNF}$ (12)	116.36 ± 3.89*	101.89 ± 7.06
5xFAD$^{ProAHN/Veh}$ (10)	100.00 ± 6.27	100.00 ± 6.87
5xFAD$^{+AHN(RUN)/Veh}$ (15)	123.13 ± 6.13*	125.74 ± 5.45*
5xFAD$^{ProAHN/AICAR}$ (15)	103.62 ± 4.16	104.48 ± 5.07
5xFAD^{Veh} (8)	100.00 ± 6.42	100.00 ± 6.71
5xFAD^{AICAR} (8)	106.23 ± 5.44	100.85 ± 4.11

Female	PSD95	IL-6
5×FAD$^{ProAHN/LV-RFP}$ (6)	100.00 ± 5.31	100.00 ± 4.40
5×FAD$^{+AHN(RUN)/LV-RFP}$ (11)	122.87 ± 4.10*	123.37 ± 5.62*
5×FAD$^{ProAHN/LV-BDNF}$ (13)	120.63 ± 5.22*	101.55 ± 5.34
5xFAD$^{ProAHN/Veh}$ (8)	100.00 ± 6.95	100.00 ± 5.76
5xFAD$^{+AHN(RUN)/Veh}$ (10)	125.92 ± 7.44*	127.53 ± 7.56*
5xFAD$^{ProAHN/AICAR}$ (10)	101.34 ± 5.58	98.85 ± 8.15

Table S9
Levels of hippocampal PSD95 and IL-6 among the different treatment groups.
In male 5×FAD$^{ProAHN/LV-RFP}$, 5×FAD$^{+AHN(RUN)/LV-RFP}$, and 5×FAD$^{ProAHN/LV-BDNF}$ mice, $F_{(2,35)} = 4.197$, $P < 0.05$ (PSD95); $F_{(2,35)} = 5.518$, $P < 0.01$ (IL-6). In male 5×FAD$^{ProAHN/Veh}$, 5×FAD$^{+AHN(RUN)/Veh}$, and 5×FAD$^{ProAHN/AICAR}$ mice, $F_{(2,37)} = 5.159$, $P < 0.05$ (PSD95); $F_{(2,37)} = 5.944$, $P < 0.01$ (IL-6). In female 5×FAD$^{ProAHN/LV-RFP}$, 5×FAD$^{+AHN(RUN)/LV-RFP}$, and 5×FAD$^{ProAHN/LV-BDNF}$ mice, $F_{(2,27)} = 4.482$, $P < 0.05$ (PSD95); $F_{(2,27)} = 5.633$, $P < 0.01$ (IL-6). In female 5×FAD$^{ProAHN/Veh}$, 5×FAD$^{+AHN(RUN)/Veh}$, and 5×FAD$^{ProAHN/AICAR}$ mice, $F_{(2,25)} = 4.866$, $P < 0.05$ (PSD95); $F_{(2,25)} = 4.922$, $P < 0.05$ (IL-6). Number of animals is indicated in parentheses.

Groups	TGF-β1
$5\times FAD^{CTL}$ (8)	100.00 ± 6.32
$5\times FAD^{ProAHN}$ (10)	116.68 ± 9.79
$5\times FAD^{+AHN(RUN)}$ (8)	96.28 ± 5.17
$5\times FAD^{\psi AHN(RUN)}$ (9)	98.05 ± 5.69
$5\times FAD^{ProAHN/LV\text{-}RFP}$ (8)	100.00 ± 5.18
$5\times FAD^{+AHN(RUN)/LV\text{-}RFP}$ (15)	94.45 ± 6.64
$5\times FAD^{ProAHN/LV\text{-}BDNF}$ (15)	107.17 ± 6.38
$5\times FAD^{LV\text{-}RFP}$ (8)	100.00 ± 4.42
$5\times FAD^{LV\text{-}BDNF}$ (12)	103.13 ± 5.34

Table S10
Effects of inducing AHN alone, AHN with BDNF, BDNF alone, or by exercise on hippocampal TGF-β1 levels.
The level of TGF-β1 in the hippocampal homogenates of male mice in the experimental groups listed in the table. Levels are presented as % of the 5×FAD control group within each treatment (top row of each table). No differences were seen between any of the groups. Number of animals is indicated in parentheses.